ADVANCED FUNCTIONAL MATERIALS
www.afm-journal.de

Bioinspired Superwettability Electrospun Micro/Nanofibers and Their Applications

Lanlan Hou, Nü Wang, Jing Wu, Zhimin Cui, Lei Jiang, and Yong Zhao**

Inspired by the self-cleaning phenomenon in nature biology, superwettable materials systems have been increasingly studied by multidisciplinary scientists in past two decades. Among various fabrication methods, electrospinning technology, with superior capability of comprehensive coordination of surface chemical composition and hierarchical micro/nanostructures, has been proved to be a versatile method to fabricate diverse fibrous materials with superwettability from polymers, ceramics, to composites. This review first introduces the progress of electrospinning technology in generating various hierarchical structured nanofibers. Then, the wetting theory of liquid on fibers and recent approaches toward fabricating bioinspired electrospun micro/nanofibers with superwettability are described. Based on the special wettability to different liquids, the electrospun nanofibrous materials play significant roles in liquid mixtures separations, water collection, unidirectional liquid penetrations, and in environmentally responsive materials. Finally, the challenges and promising prospects on electrospun superwettability nanofibrous materials are highlighted.

1. Introduction

Nature has revealed its perfect designing performances of biomaterials with fascinating structures and optimized functions through millions of years of evolution. According to the achieved progresses in biomimetic field, learning from nature has been demonstrated as an effective way to develop various functional materials.[1–5] Superwettability system is an outstanding representative of bioinspired materials. As the ancient Chinese saying goes, that "the lotus rises from the mud but is not stained," it describes the natural self-cleaning phenomenon of lotus leaves when coming out from dirty water. This well-known self-cleaning "lotus effect" is due to the superhydrophobicity (water contact angle (WCA) higher than 150°) of its surface.[6–8] Besides lotus leaves, there are many other superwettability phenomena in nature, such as anisotropic wetting property of rice leaves[9] and some waterfowl feathers,[10,11] superhydrophobic water strider's legs,[12–14] gradient wettability of spider silk,[15,16] cactus spines,[17] nepenthes,[18,19] etc. In the past two decades, researches have revealed that surface free energy and micro/nanoscale structures are the two main determinants of material superwettability. Many methods have been developed to fabricate superwettability materials, such as sol–gel method,[20,21] chemical vapor deposition,[22–24] surface grafting,[25–28] etching,[29–32] plasma treatment,[33–35] electrochemical methods,[36–39] self-assembly,[40–43] layer-by-layer method,[44,45] template method,[46–48] solvent–nonsolvent technique,[49,50] electrospinning,[51–53] etc. Among these approaches, electrospinning technique, a technique that generates nanofibers by stretching viscous polymeric solution under high voltage electrostatic force, exactly meets the two requirements to prepare materials with regulated chemical composition and hierarchical micro/nanostructures.[54–56] On one hand, various polymeric or inorganic/organic composite materials with required surface energy could be electrospun to nanofibrous materials. On the other hand, the electrospinning method possesses powerful structural tunability that could create fibers with microscale hierarchical structures. **Scheme 1** shows the outline of this review. The structures of the electrospun nanofibers could be well tailored from microscopic to macroscopic. It means we can control not only various outer and inner structures of nanofibers, but also different nanofibers assemblies from 1D yarn to 2D film to 3D block. These diverse structured nanofibers show superwettability such as superhydrophobic, superhydrophilic, superoleophobic, and superoleophilic. By virtue of the special structures and wettability, they can be used for many applications. It is delightful to see that the intersection of these two rapidly evolving fields, superwettability surfaces and electrospinning technology, has generated a

Dr. L. Hou, Prof. N. Wang, Prof. Z. M. Cui, Prof. L. Jiang, Prof. Y. Zhao
Key Laboratory of Bioinspired Smart Interfacial Science
and Technology of Ministry of Education
Beijing Key Laboratory of Bioinspired Energy Materials and Devices
School of Chemistry
Beijing Advanced Innovation Center for Biomedical Engineering
Beihang University
Beijing 100191, P. R. China
E-mail: wangn@buaa.edu.cn; zhaoyong@buaa.edu.cn
Prof. J. Wu
Beijing Key Laboratory of Clothing Materials R&D and Assessment
Beijing Engineering Research Center of Textile Nanofiber
School of Materials Science and Engineering
Beijing Institute of Fashion Technology
Beijing 100029, P. R. China
Prof. L. Jiang
Key Laboratory of Bio-inspired Smart Interface Science
Technical Institute of Physics and Chemistry
Chinese Academy of Sciences
Beijing 100190, P. R. China
The ORCID identification number(s) for the author(s) of this article can be found under https://doi.org/10.1002/adfm.201801114.

DOI: 10.1002/adfm.201801114

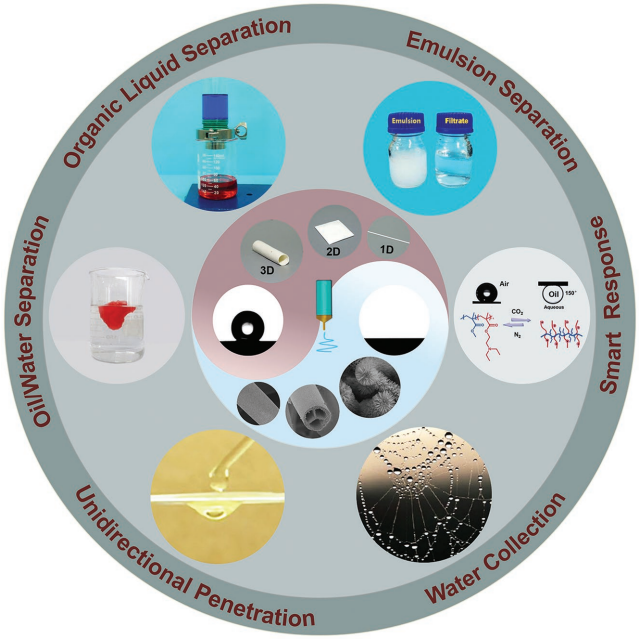

Scheme 1. The electrospun multi-structured superwettability nanofibers and their applications. The nanofibers could be well-tailored with various outer and inner microscopic structures as well as different assembly configuration of 1D–3D. These nanofibrous materials are of special wettabilities, such as superhydrophobic, superhydrophilic, superoleophobic and superoleophilic, which have been widely used in self-cleaning, oil/water separation,[236] organic liquid separation,[144] emulsion separation,[195] smart responsive surface,[234] water collection,[204] and unidirectional penetration[216] etc. Reproduced with permission.[236] Copyright 2015, Elsevier. Reproduced with permission.[144] Copyright 2016, Lanlan Hou et al., Published by Springer Nature. Reproduced with permission.[195] Copyright 2018, Wiley-VCH. Reproduced with permission.[234] Copyright 2015, Wiley-VCH. Reproduced with permission.[204] Copyright 2014, American Chemical Society. Reproduced with permission.[216] Copyright 2015, Wiley-VCH.

lot of interesting new materials with various structures and special properties in a wide range of applications. In this review, first, we briefly introduce the formation mechanism of some representative hierarchical structured fibers by electrospinning. Then, we discuss the bioinspired fabrication of superwettability materials by electrospinning and their wetting mechanism. In the third part, we focus on the applications of electrospun superwettability micro/nanofibers such as self-cleaning, oil/water separation, organic liquid separation, emulsion separation, smart responsive surface, water collection, unidirectional penetration, etc. Finally, we provide a summary and outlook for the future in the fields.

2. Multistructured Electrospun Micro/Nanofibers

Electrospinning is a technique that uses electrostatic force to produce ultrafine fibers with diameters ranging from a few nanometers to several micrometers. Anton first applied a series of patents on the set-up for fabricating polymer filaments by electrostatic force in 1934.[57] In 1966, Simons used an electrospinning apparatus to fabricate very lightweight, ultrathin nonwoven fibers.[58] It was found that the fibers from low viscosity solutions tended to be shorter, while the fibers from more viscous solutions would be longer and relatively continuous. In 1971, Baumgarten reported electrospun acrylic fibers with diameters in the range of 0.05–1.1 µm.[59] Nevertheless, these developments did not attract much attention because of the limitations of high voltage technique and nanoscale characterization technique. In 1990s, accompanied with the flourishing of nanotechnology, the electrospinning technique had been rapidly developed

Lanlan Hou is currently a Ph.D. student at the School of Chemistry, Beihang University, in the group of Professor Yong Zhao and Associate Professor Nü Wang. She received her B.S. degree (2013) in Applied Chemistry, from Hebei Normal University, China. Her present research interest is focused on electrospinning nanofiber materials with special wettability.

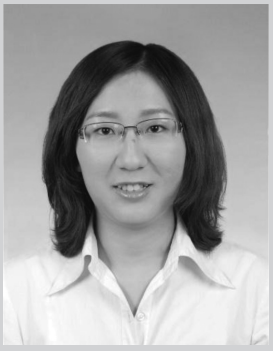

Nü Wang received her B.S. degree (2004) from Jilin University and Ph.D. degree (2009) in Physical Chemistry from Institute of Chemistry, Chinese Academy of Sciences. From 2009 onward, she was a faculty member in School of Chemistry, Beihang University. She has been an associate professor since 2017. Her study is focused on functional micro/nanostructured materials by electrospinning and their properties.

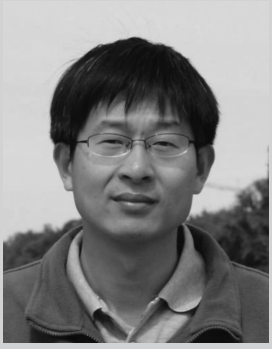

Yong Zhao is currently a professor at the School of Chemistry, Beihang University. He received his Ph.D. from the Institute of Chemistry, Chinese Academy of Sciences (ICCAS), China in 2007 (with Prof. Lei Jiang). He worked at ICCAS from 2007–2011 and then moved to Beihang University in 2011. During 2016–2017, he worked as a visiting scholar at Harvard University with Prof. David A Weitz. His research focuses on the fabrication of multistructured nanofibers by electrospinning and their applications in membrane separation, catalysis, etc.

due to its advantages of being simple and powerful to fabricate ultrafine fibers down to nanoscale. In 1995, Doshi and Reneker pointed out that many parameters can influence the transformation of polymer solutions into nanofibers during the electrospinning process, including solution properties, the electrical potential, ambient parameters, etc.[60,61] After decades of development, electrospinning technology has achieved fruitful results and significant progresses. The electrospinning technique exhibited its tremendous ability in generating diverse kinds of hierarchical micro/nanostructures. **Figure 1** presents an overview of some typical outer structures and inner structures of electrospinning micro/nanofibers.

2.1. Multiscale Outer Structures

Figure 1a shows a simple cylindrical fiber, which is the most representative and common structure of electrospinning product.[62] Normally, many linear macromolecules can be electrospun into such cylindrical fibers when they are dissolved in a suitable polar solvent with proper concentration (Figure 1a). Besides cylinder shape nanofibers, there are two other structures that are frequently available by electrospinning, which are ribbon-like oblate fiber (Figure 1b) and periodic bead-on-string fiber (Figure 1c).[63,64,72] Although the structures of these three kinds of fibers seem quite different, the underlying formation mechanism of them is same. As mentioned, if proper concentration of spinning solution is used, cylinder fibers would be produced. Actually, the formation of fiber is a balance of viscoelasticity and Rayleigh instability. In the absence of external force, a viscous liquid will spontaneously shrink to spherical shape under surface tension. During electrospinning process, however, the viscous liquid was stretched into a very thin stream to reduce the electrostatic repulsion under the Coulomb force. On the contrary, the Rayleigh instability at the fluid interface will lead to a dynamic shape deformation on fibers. In this case, the viscoelasticity inclines to sustain the cylindrical shape of stream, while the Rayleigh instability tends to deform the cylindrical stream into wave stream or even breaks up to smaller droplets in order to acquire less surface area (thermostability state). The final shape configuration of the fibers is decided by the balance of these two forces. Thus, there are three possible situations. First, the spinning solution is of suitable concentration, the cone jet will be quickly stretched to very thin stream, and the solvent evaporates synchronously. With the solidification of liquid stream, cylindrical fibers are generated, as Figure 1a indicated.[62] Second, if the concentrated spinning solution with high viscoelasticity is electrospun, the electrostatic force could only stretch the solution jet into stream with relative large diameter (normally tens of micrometers). Owing to the large diameter, the solidification of the stream is not synchronous that it will form a solid shell but leave a liquid core inside the fiber. With the further evaporation solvent, the volume of core shrinks so that ribbon-like fiber can be obtained caused by the collapse of the shell. As a result, cylindrical fibers deform to flat ribbon-like fiber. In these two cases, viscoelasticity plays a dominant role in shape forming, while Rayleigh instability is neglectable. Third, when the dilute spinning solution with low viscosity is

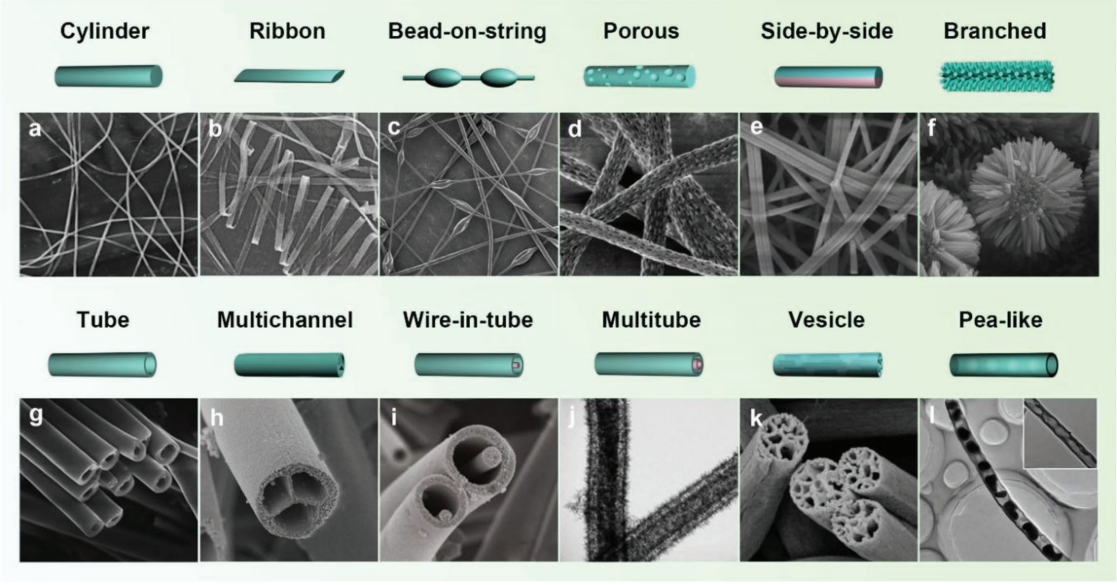

Figure 1. Micro/nanofiber with multi-structures by electrospinning technique. a) cylinder structure,[62] b) flatted ribbon structure,[63] c) bead-on-string structure,[64] d) surface porous structure,[65] e) side-by-side structure,[66] f) branched structure, g) tube structure,[67] h) multichannel structure, i) wire-in-tube structure,[68] j) multiwall structure,[69] k) vesicle structure,[70] and l) pea-like structure.[71] It shows the versatility of the electrospinning technique. Reproduced with permission.[62] Copyright 1999, Elsevier. Reproduced with permission.[63] Copyright 2001, Wiley-VCH. Reproduced with permission.[64] Copyright 2012, Wiley-VCH. Reproduced with permission.[65] Copyright 2001, Wiley-VCH. Reproduced with permission.[66] Copyright 2007, American Chemical Society. Reproduced with permission.[67] Copyright 2004, American Chemical Society. Reproduced with permission.[68] Copyright 2010, American Chemical Society. Reproduced with permission.[69] Copyright 2014, American Chemical Society. Reproduced with permission.[70] Copyright 2011, Wiley-VCH. Reproduced with permission.[71] Copyright 2015, Chaojiang Niu et al., Published by Springer Nature.

adopted, the viscoelasticity is easy to be concurred. Then Rayleigh instability governs the shape of stream so that fluctuation emerges on cylindrical stream and finally forms periodic spindle shaped fiber after solidification (Figure 1c). Fong et al. investigated fiber morphologies with polyethylene oxide (PEO) in different concentrations.[62] They found that higher polymer viscosity leads to fewer beads. The morphology of the beads changed from spherical to spindle-like when the concentration of the polymer varied from low to high level. Xia and co-workers reported that the density of beads was reduced with increasing concentration of polyvinyl pyrrolidone (PVP).[73] Meanwhile, the introduction of a small amount of salt would avoid the formation of beads on the nanofibers. Vancso and co-workers discovered that electrospun PEO fibers vary different bead morphologies when different solvents were used.[74] Besides fiber shape controllability, electrospinning is of capability of tuning fiber's surface microstructures and compositions. For example, bumped or porous fibers could be fabricated by using some water immiscible hydrophobic polymers. As known, the electrospinning is often operated at air environment with inevitable humidity. Because the stretched solution is of quite large specific area, the solvent will rapidly evaporate and take away heat. It results in the lower temperature of jetting stream than environment. Therefore, moisture will condense to numberless tiny water droplets at surface of low temperature jetting stream. If the spinning system is hydrophobic water immiscible polymer, microphase separation will occur on the sites where the tiny droplets condensed. As a result, these water droplets positions will leave cavity or pores and form porous fibers ultimately (Figure 1d). Wendorff and co-workers used dichloromethane as solvent to fabricate poly-L-lactide (PLLA) fibers, polycarbonate fibers, and polyvinylcarbazole fibers, which are characterized by regular pores or pits in the 100 nm range (Figure 1d).[65] The surface porosity is attributed to the rapid phase separation induced by the evaporation of the solvent and a subsequent rapid solidification. Rabolt and co-workers introduced polymeric fibers with several types of porous morphologies, with pore diameters in the range of 20–350 nm to 1 μm.[75] Then, they investigated the influence of the processing parameters on the porous morphology of polystyrene (PS) electrospun fibers, including the solvent vapor pressure and the relative humidity. The rapid solvent evaporation responsible for the pores most likely occurs due to evaporative cooling of the polymer solution, as it travels the distance from the syringe to the collector, inducing the formation of pores. Han and co-workers explored the construction of hierarchical structured PS fibers by electrospinning.[76] They recognized that solvents, environmental humidity, temperature, etc., would affect the hierarchical structures on the fibers. Above mentioned strategy could generate various structures of homogeneous materials. Electrospinning technique could also be used to fabricate heterogeneous nanofibers by direct or indirect route. For example, a juxtaposed spinneret could be employed to produce heterostructured Janus side-by-side nanofibers, as Figure 1e indicated.[66] Another heterogeneous strategy is to use electrospun nanofibers as substance, on which secondary structured heterogeneous materials could be created such as pine-branch-like structures, as shown in Figure 1f.

2.2. Multiscale Inner Structures

Engineering the complex hierarchical nanostructures has been recognized as an important route to endow functions for many applications. Electrospinning is such a technique that could generate nanofibers with complex inner structures including core/sheath, hollow, and more complex structures[77] The coaxial electrospinning technology is a turning point of electrospinning that opens the door of designing complex structured fibers. In 2002, Loscertales et al. proposed an electro-hydrodynamic coaxial jetting method to produce microcapsules.[78] Then this newfangled technology was soon applied to generate continuous core–shell fibers, which was named coaxial electrospinning (or simplified as co-electrospinning).[79–82] The conventional electrospinning set-up with one spinneret is usually used to manufacture solid fibers with one component or a mixture of components. Coaxial electrospinning has exhibited outstanding performances to construct various multilevel structured fibers beyond the traditional electrospinning. In coaxial electrospinning, the compound spinneret consists of a thinner capillary coaxially placed inside a thicker capillary. Two immiscible liquids are fed separately through the two capillaries in an appropriate flow rate, and they will form a compound Taylor cone jet on the tip of the coaxial outlet. After the solidification of the outer liquid, a core–shell fiber or a liquid-filled hollow fiber can be obtained. Loscertales et al. first generated hollow nanotubes by one-step coaxial electrospinning.[78,83] In addition, Li and Xia have prepared the TiO_2 hollow nanofibers combined the coaxial electrospinning technique with the sol–gel method, as shown in Figure 1g.[67] Yarin and co-workers prepared polysulfone/PEO and poly(dodecylthiophene)/PEO core–shell polymer nanofibers by coaxial electrospinning.[84] To be mentioned, the poly(dodecylthiophene) could not be electrospun into fibers itself due to low molecular weight. That is to say, the co-eletrospinning has benefitted to expand the materials of choices, especially some functional agents cannot form fiber themselves. Based on the routine coaxial electrospinning method, many further developments of electrospinning have emerged recently, such as multifluidic compound-jet electrospinning and multifluidic coaxial electrospinning. Accordingly, various multilevel structured fibers, especially with inner hierarchical structure, have been obtained. In 2007, we developed a novel multifluidic compound-jet electrospinning method to fabricate multichannel microtubes in one step (Figure 1h).[85] The experimental setup is characterized by two or more capillaries embedded in a blunt metal needle. The immiscible inner fluids and outer fluids were separately fed into the capillaries and the blunt metal needle with an appropriate flow rate. It could form multicomponent or multichannel core–shell fibers. The number of core components could be controlled by flexibly adjusting the number of inner capillaries.[86] In addition, we also reported an improved multifluidic coaxial electrospinning method to fabricate nanowire-in-microtube structured core–shell fibers (Figure 1i).[68] It was obtained by introducing an extra middle fluid into the compound spinneret as a spacer for the outer and inner layers of fibers. Then, three-layered core–shell fibers were formed by highly miscible or microphase separation solutions with the middle fluid as a spacer. With subsequent selective removing the middle spacer fluid between the sheath and the core materials, heterogeneous wire-in-tube structured fibers

were prepared. These works demonstrated that multistructured hollow nanofibers could be produced by rationally designing the configuration of spinneret. This could be regarded as a physical route. Actually, chemical route is also developed to create multistructures. Xing and co-workers reported that a single-capillary electrospinning could generate hollow double-walled nanofibers (Figure 1j).[69] In the hydrothermal process, SiO_2 served as nucleation point for simultaneous growth of copper silicate nanofibers on both the inner and outer surfaces, then the double-walled structure copper silicate hollow nanofibers were prepared, as the SiO_2 sacrificial layer was removed. Interior porous structures can be also controlled by adjusting the experimental parameters via electrospinning.[87] Xia and co-workers prepared porous PS and polyacrylonitrile (PAN) fibers through electrospinning the liquid jet into a collector immersed in cryogenic liquid.[88] In the electrospinning process, the remaining solvent along the fibers is frozen in the liquid nitrogen bath before reaching the collector. Phase separation into solvent-rich and solvent-poor regions takes place in the freezing process, which would induce porous morphology by controlling the solvent evaporation. Peng et al. presented nanoporous structured, submicrometer carbon fibers via electrospinning of PAN and a copolymer of acrylonitrile and methyl methacrylate in dimethyl formamide.[89] Microphase-separated domains occurred during electrospinning because of the rapid solvent evaporation and solidification of the electrospun fibers. Then, the copolymer domains resulted in porous structure in the fibers in the course of oxidation, which could be preserved after carbonization.[90] Recently, we developed a versatile microemulsion electrospinning method to fabricate ultraporous nanofibers with hierarchical interior structures (Figure 1k).[70] The microemulsion solution composed of metal alkoxide and paraffin oil could be easily electrospun into nanofibers. After calcination and selective removal of the oil phase, the hybrid nanofibers decomposed to porous inorganic nanofibers. The interior structures of the fibers were governed by the tiny oil droplets in the microemulsion, which served as soft templates and could be easily controlled by changing the experimental parameters, such as the composition of the microemulsion and the emulsification conditions.[86] Mai and co-workers fabricated peapod-like hollow nanofibers by a gradient electrospinning and controlled pyrolysis method (Figure 1l).[71] Above works prove that electrospinning is a very competitive approach for well-controllable generating of nanofibrous materials with a good variety of structures and composition. This outstanding advantage facilitates its many applications in broad fields such as gas filter, functional textile, battery and supercapacitors, drug release and tissue-regeneration, as well as superwetting materials.[91–94] Here, we focus on the blossoming progress of superwettability nanofibers and their applications.

3. Superwettability Electrospun Micro/Nanofibers

3.1. Wetting Behavior on Flat Surfaces and Fibers

Wetting is one of the most important properties of a solid substrate, which is governed by the surface free energy and micro/nanoroughness. As mentioned, electrospun nanofibers could be of diverse compositions and microstructures, they thereby show many special wetting properties. Here, we briefly describe the wetting mechanism of 2D flat surfaces and 1D fibers. The most familiar examples are that water can spread on glass, while mercury will form a spherical drop on glass. The former is defined as "wetting," and the latter is "nonwetting." Generally, the surface free energy and the surface microstructure are two dominant factors that affect the wettability of solid surfaces.[3,95–97] For a liquid droplet on a flat solid substrate, its wetting behavior is determined by the solid surface free energy (γ_{sg}), the liquid surface tension (γ_{lg}), and the interfacial free energy of solid and liquid (γ_{sl}), which are the intrinsic properties of materials and liquid. In 1805, Young proposed the equation $\gamma_{sg} = \gamma_{sl} + \gamma_{lg}\cos(\theta)$ that first described the intrinsic contact angle (CA, θ) of a liquid droplet on an ideal flat solid surface at a thermodynamic equilibrium state (**Figure 2**a).[98] In fact, the surface microstructure or roughness is another key factor that has important influences

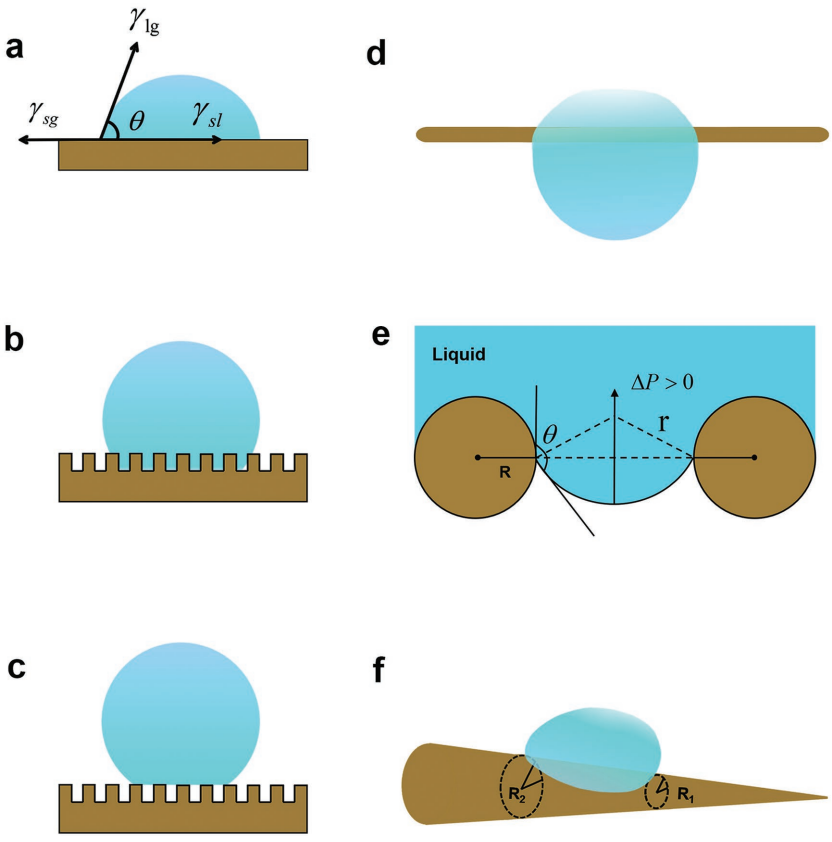

Figure 2. Wetting model of 2D flat surfaces and 1D fiber surfaces. Drop on a) the flat smooth surface, b) hydrophobic flat rough surface (Wenzel's state), and c) superhydrophobic flat rough surface (Cassie–Baxter state). The droplet on d) a single fiber, e) nonwoven electrospinning fibrous membrane, and f) asymmetric structure fiber.

on the wettability of solid surfaces.[99] In 1936, Wenzel further proposed an amplification theoretical model that roughness resulted effect on wettability, as illustrated in Figure 2b. It defines the relationship between the contact angle of a water drop on a rough surface of various hierarchical morphologies (θ_r) and the intrinsic CA of a water drop on a flat surface.[100] In this equation, $\cos(\theta_r) = r\cos(\theta)$, r is the roughness factor, which is defined as the ratio of the actual solid/liquid interface contact area to the area of a smooth, flat surface with the same dimensions. The r is always greater than 1 for a rough surface. The surface will become more hydrophilic with surface roughness increased, if the water CA on the flat surface is smaller than 90°. Accordingly, if the water CA on the flat surface is greater than 90°, the surface will become more hydrophobic with increasing roughness of the surface. Enhancement on rough structure of surfaces will significantly affect the wettability. In 1944, Cassie and Baxter extended the assumption of Wenzel and proposed that a rough surface should be considered as an air-solid heterogeneous composite surface for a highly hydrophobic material.[101] In the Cassie model, the water droplet could not completely contact with the entire surface because air pockets are trapped between the grooves of the rough surface, as shown in Figure 2c. The contact angle in such state is given by the Cassie–Baxter equation, $\cos(\theta_r) = -1 + f[\cos(\theta) + 1]$, where f is defined as solid area fraction of the substrate in contact with the liquid droplet, and $((1)–f)$ is the area fraction of the trapped air.

The above theoretical descriptions are the class wettability mechanisms normally for the solid surface. However, as for a single nanofiber or few fibers, the wetting behavior is a 1D wetting model, which is quite different from 2D flat surface wetting. Therefore, it is necessary to describe the wetting behavior of droplets on 1D fiber object. The most important feature of 1D fiber wetting different to 2D flat surface is that the drop is located on a high curvature surface. The radius of curvature of thin fiber is usually close to the droplet diameter. The wetting scenario could be abstracted to three models. Case-1 is the droplet hanging on a single cylindrical fiber.[102–104] Here, a balance between gravity and capillary forces should be considered for a hydrophilic fiber. For a smaller droplet on a fiber, when the gravity is less than or equal to the capillary force, the droplet shows a symmetrical spherical shape. With the increasing of droplet volume and influence of gravity, the gravity of a bigger droplet cannot be balanced by the capillary force, the spherical shape is deformed, and the droplet tends to form an asymmetric shape, as shown in Figure 2d. When the droplet cannot be holded by the fiber, the droplet eventually will depart away under the force of gravity. In general, large amount of electrospun nanofibers will interweave to a nanofibrous mat, which is a porous membrane with large roughness. Case-2 illustrates a droplet hanging between two hydrophobic fibers (Figure 2e), which is a simplified nonwetting model of liquids on large number of lyophobic fibers.[99,105,106] When a droplet is hanging between two fibers with a CA larger than 90°, it will form a meniscus shape. The curvature generates an upward pressure, ΔP, that prevents the droplet crossing from the two fibers. The ΔP in Equation (1) can be expressed as

$$\Delta P = \frac{2\gamma_{lg}}{r} = \frac{4\gamma_{lg}\cos\theta}{d} \quad (1)$$

For the lyophobic cylindrical fiber, the R is the fiber radius and r is the curvature radius of meniscus, while d is the distance of the cross section center of the adjacent fibers. Only when the external applied pressure is bigger thanΔP, the nonwetting phase can permeate through the fibrous membranes. While the droplet with a CA lower than 90° between the fibers, there will be a downward Laplace pressure force. The wetting liquid can permeate through the membrane spontaneously without any external force. Above two cases describe the force analysis of droplet on symmetric structured fibers. If the fiber is of asymmetric conical shape (Case-3), it will generate a nonequilibrium Laplace pressure that could drive the directional motion of droplet (Figure 2f).[16,107,108] This is the reason why spider silk and cactus could collect water from fog and it is also applicable for spindle shaped nanofibers, as mentioned in Section 2.1.[17,109] The Laplace pressure driving a droplet on a conical shaped fiber with curvature structure can be expressed in Equation (2)

$$\Delta P_{Curvature} = -\int_{R_1}^{R_2} \frac{2\gamma_{lg}}{(R + R_0)^2} \sin\alpha dz \quad (2)$$

Here R is the local mean radius of the fiber, R_0 is the radius of the droplet,$\alpha$is the cone hemi-angle of the conical spine, and dz is the incremental radius of the spine. The local radii along a conical fiber at the two opposite sides are donated as R_1 and R_2, respectively. It explains the dynamics of a drop placed on a conical fiber; the structure gradient of the conical fiber makes the droplet spontaneously move from high curvature region (thinner tip) toward low curvature region (thicker tip). In fact, the traditional Chinese brushes exactly take advantage of droplets on the conical fibers, so as to making the brush with excellent capacity for holding ink.[110] When the brush is dipped in ink, the ink will self-propell the movement under the Laplace pressure gradient from the "two parallel fibers" system, until they reach a region where Laplace capillary force and gravity force equilibrate. These mechanisms describe wetting property of electrospun products with different structures such as fibrous membrane (2D model) and few fiber(s) wetting (1D), which is helpful to comprehend and rationally design superwettability electrospun materials.

3.2. Bioinspired Superhydrophobic Surface

After millions of years of evolution, nature creatures have exhibited increasingly perfect functions. These findings brought us many new strategies to design and fabricate superwettability materials. Inspired by nature, great progress has been made in the bionic preparation of superhydrophobic artificial surfaces through structural or property biomimetic. Here, we briefly describe the preparation of superwetting surface materials by electrospinning.

Inspired by self-cleaning lotus leaves in **Figure 3**a,b,[7,8,119,120] we fabricated a lotus-leaf-like superhydrophobic surface with porous microspheres and nanofibers in a composite structure by electrospinning. The morphology of the electrospun PS products could be controlled by the concentration of the precursor solutions. The porous microspheres were found to play a leading role in the superhydrophobicity. At the same time,

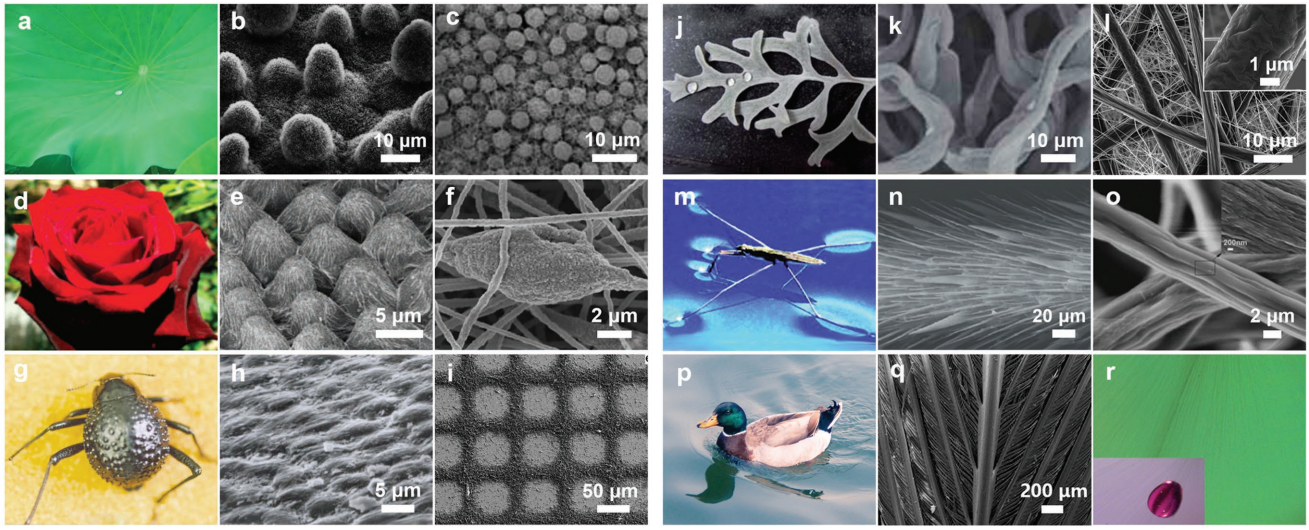

Figure 3. The superhydrophobic surfaces from nature and the nature inspired artificial superhydrophobic materials. a) superhydrophobic lotus leaves b) surface microstructures on lotus leaf.[8] c) superhydrophobic PS films with microspheres and nanofibers composite structures.[51] d,e) superhydrophobic high adhesive rose petal and its microstructures.[111] f) superhydrophobic high adhesive fluorinated polyimide mat.[112] g,h) desert beetle's back with incorporates hydrophobic and hydrophilic regions, which could collect water from fog.[113] i) The hydrophobic and superhydrophilic patterned surface prepared by electrospinning, photolithographic and pyrolysis.[114] j,k) superhydrophobic silver ragwort leaf surface composed of microfibers.[115] l) electrospun fibrous mats.[116] m) water strider on the water surface.[14] n) water strider leg with oriented spindly microsetae.[13] o) The artificial strider-leg-like POSS-PMMA fibers.[117] p) The duck feather shows a superhydrophobic surface and q) a fan radial shape. r) Water droplets set on a fan-shaped radiating electrospun nanofiber pattern surface.[118] It is seen that some electrospun materials have well-mimicked both structures and functions of natural biology. Some others electrospun products are bio-functional mimic instead of structural mimic. Reproduced with permission.[8] Copyright 1997, Springer Nature. Reproduced with permission.[51] Copyright 2004, Wiley-VCH. Reproduced with permission.[111] Copyright 2008, American Chemical Society. Reproduced with permission.[112] Copyright 2012, Royal Society of Chemistry. Reproduced with permission.[113] Copyright 2001, Springer Nature. Reproduced with permission.[114] Copyright 2010, American Chemical Society. Reproduced with permission.[115] Copyright 2011, Royal Society of Chemistry. Reproduced with permission.[116] Copyright 2009, American Chemical Society. Reproduced with permission.[14] Copyright 2007, American Chemical Society. Reproduced with permission.[13] Copyright 2004, Springer Nature. Reproduced with permission.[117] Copyright 2009, Royal Society of Chemistry. Reproduced with permission.[118] Copyright 2008, Royal Society of Chemistry.

the nanofibers linked the individual microspheres together and reinforced the composite films (Figure 3c). This is the beginning of fabrication superwettability materials by electrospinning.[51] Then some lotus-leaf-structured or similar hierarchical structured surfaces with superhydrophobicity have fabricated electrospinning.[121,122] For example, superhydrophobic poly(ε-caprolactone) (PCL) surfaces with micrometer-sized pyramidal structures consisting of accumulated droplets and nanofibers were obtained using a one-step modified electrostatic process.[123] Ding and co-workers fabricated biomimetic superhydrophobic fibrous mats by electrospinning the PS solution in the presence of silica nanoparticles, which exhibited a fascinating structure with a combination of nanoprotrusions and numerous grooves.[115,124] Jin and co-workers studied the wettability of electrospun fibers made from PS solutions with different solvents of tetrahyrofuran and chloroform.[125] The water CAs on the mat surfaces depended on the surface morphology. Rutledge and co-workers introduced two approaches to preparing double-roughened superhydrophobic fabrics by electrospinning, one is directly introducing nanometer-scale pore structure onto electrospun fiber surfaces, another is decorating the as-prepared fibers with fine nanoparticles using a layer-by-layer deposition technique, both produced highly stable superhydrophobic fabrics.[126]

Besides the "lotus effect," there is another superhydrophobic phenomenon in nature, denoted as the "petal effect." It means that the surface presents a water CA larger than 150° and high adhesion at the same time.[127,128] Figure 3d,e presents the optical picture and scanning electron microscope (SEM) image of an ordinary red rose petal.[111] There are periodic arrays of micropapillae on the petal surface and further nanowrinkles on each papillae, these make the petal surface of sufficient roughness for superhydrophobicity. The water can completely occupy the micropapillae but partially infuses into the nanowrinkles, showing a Cassie impregnating wetting state. The increasing of contact surface area resulted in contact angle hysteresis and high adhesive force. Getting inspiration from the high adhesive rose petal, we have designed a fluorinated polyimide bead-on-string film, which also displayed superhydrophobic and high adhesive properties (Figure 3f).[112] The water will not roll off from the surface even when turning the film upside down.

In addition to the simple hydrophobic surface, some biological surfaces in nature are found to have the ability for water transportation. These kinds of organisms usually possess anisotropic wettability, which is derived from their unique structures on micro/nanometer scale.[15,17,129–133] Some beetles surviving in the Namib Desert can collect water from fog by their backs.[113] As demonstrated in Figure 3g,h, the desert beetle's back incorporates alternating wax-coated hydrophobic region and nonwaxy hydrophilic regions. The tiny water droplets in the fog condensations collect on its back and then transport along the hydrophobic crevices to its mouth controlled by structure

dimensions and surface energy gradient, so it can achieve the purpose of water harvesting and transportation for survival. Inspired by the beetles' back, Sharma et al. reported a strong hydrophobic and superhydrophilic patterned surface by electrospinning, photolithographic, and pyrolysis (Figure 3i).[114]

Similar to the lotus leaf, the silver ragwort is also a plant with water-repellent and self-cleaning properties. The silver ragwort leaf shows superhydrophobicity with a water CA of 147° (Figure 3j,k).[115] The SEM demonstrated that the leaf surface is covered with curved fibers and grooves along the fiber axis. The hierarchical micro/nanostructure is the key factor for the high hydrophobicity. Inspired by silver ragwort leaf, Ding and coworkers reported a biomimetic superhydrophobic surface with low surface free energy PS microfibers to produce inherent hierarchical roughness surface in Figure 3l.[115,116] Gu et al. fabricated superhydrophobic and light-shielding surfaces by endowing PS with trichome-like structures by electrospinning, inspired by the trichomes on the surfaces of silver ragwort.[134]

Water striders are a kind of insect that have remarkable nonwetting legs that enable them to stand and move freely on water. The legs are covered by large numbers of microsetae with fine nanogrooves, which, combined with the wax layer on the legs, induce the strong water resistance (Figure 3m,n).[13,14] Lin and co-workers reported the electrospinning of polyhedral oligomeric silsesquioxane-polymethylmethacrylate (POSS-PMMA) copolymer into uniform fibers that showed a water CA higher than 160° and a very low hysteresis, as inspired by the water striders' legs (Figure 3o).[117] Wu et al. fabricated an artificial water strider utilizing tiny polymer fibrils.[118] The as-prepared artificial water strider made by attaching four nanofiber-wrapped silver wires and copper strip can float on the water surface. The air was trapped in spaces between the microstructures, forming a cushion at the leg–water interface, which could strengthen the water repellence of the artificial water strider leg.

On a goose or duck feathers surface, the water droplets can only roll outward along the vein rather than moving inward and perpendicularly to the vein (Figure 3p,q).[10,11,135,136] To mimic the natural anisotropic structured surfaces, Wu et al. prepared feather-like poly(vinyl butyral) fibrous mats by redesigning the collector in the electrospinning set-up.[118] Figure 3r illustrates water dropped on a goose feather-like radiating nanofibers surface, and the water droplet was patterned with a streamlined shape. The examples demonstrate that the fabrication of superhydrophobic/amphiphobic surfaces has mainly three approaches: i) directly preparing low-surface-energy materials into desired rough structure; ii) modifying low-surface-energy materials on rough structure; iii) roughening the surface of low-surface-energy materials. The superhydrophobic materials have also been prepared by combining electrospinning with other post-treatment methods, facilitating the generation of hierarchical structures.[22,28,53] Based on understanding the complementary roles of the chemical composition and the microstructures surfaces, a booming of high performance biomimetic materials was reported.

3.3. Superoleophobic Surfaces

Above sections have demonstrated that natural superhydrophobic surfaces have showed excellent performance for water environment. However, biological surfaces with ability of superoleophobic in air have not been found so far. The artificial superoleophobic surface is such a typical example that is from nature but beyond nature. Up to now, the superoleophobic surfaces can be divided into air superoleophobic and underwater superoleophobic.[137–143] The difficulty of air superoleophobic materials lies in that the organic liquids possess much lower surface tension than water. It means much lower surface free energy materials need to be explored. Cohen and co-workers revealed how a re-entrant surface curvature displays extreme resistance to oil in conjunction with chemical composition and roughened surface.[146] They synthesized a class of low-surface-energy polyhedral oligomeric silsesquioxane molecules. The PMMA and fluorodecyl POSS blend with beads-on-strings structures were fabricated by electrospinning (**Figure 4**a), which exhibited superhydrophobic properties with large CAs.[136] Moreover, the θ^*_{adv} and θ^*_{rec} of liquids with different surface tensions demonstrated that the surfaces became even superoleophobic with increasing mass fraction of POSS (Figure 4b). Recently, we reported a flexible wettability-tunable nanofibrous membrane composed of a poly(vinylidene fluoride-co-hexafluoropropylene (PVDF-HFP) as the matrix and fluorosilane (PFDTMS) as a surface energy regulator.[144] Figure 4c shows the morphology of PVDF-HFP nanofibrous membranes. Figure 4d showed that the oil-repellent ability could be continuously increased with the decreasing of surface energy. Han and Steckl produced core–sheath structured oleophobic and superhydrophobic fibers through coaxial electrospinning.[145] The Teflon AF, which is normally not electrospinnable but is a widely used hydrophobic material, was used as sheath material, and gelatin or PCL was used as core material (Figure 4e). The coaxial electrospun PCL/Teflon fiber membrane shows an amphiphobic performance that produced a water CA of 158° as well as a rolling angle of ≈5° and a dodecane CA of ≈130°. Figure 4f illustrates that the water can even bounce when impact is on the coaxial fiber membranes. This method provides another way for non-electrospinnable material such as Telfon AF, which could be electrospun when combined with electrospinnable core materials by coaxial electrospinning, which provides inspiration for designing lyophobic materials by electrospinning. Besides air superoleophobic, many marine animals show a superoleophobic property underwater.[147] Inspired by the oil-repellent surface of fish skin, the underwater superoleophobic surfaces are achieved through the chemical or physical decoration of hydrogel or another liquid phase.[148–151]

3.4. Superhydrophilic Surface

In contrast to the lyophobic surfaces, relatively small studies were conducted to intentionally produce the superhydrophilic surfaces by electrospinning. This is because for most of the electrospinning lyophilic materials, they often show a direct "superlyophilicity" toward liquid due to the fast absorption of droplets by its porous structure.[156] But it is notable that it is not very accurate to say a porous hydrophilic media "superhydrophilic" because the liquid is soaked rather than spreading on the surfaces. Wang et al. fabricated a superhydrophilic TiO_2 fibrous mesh with an ultrafast spreading property by

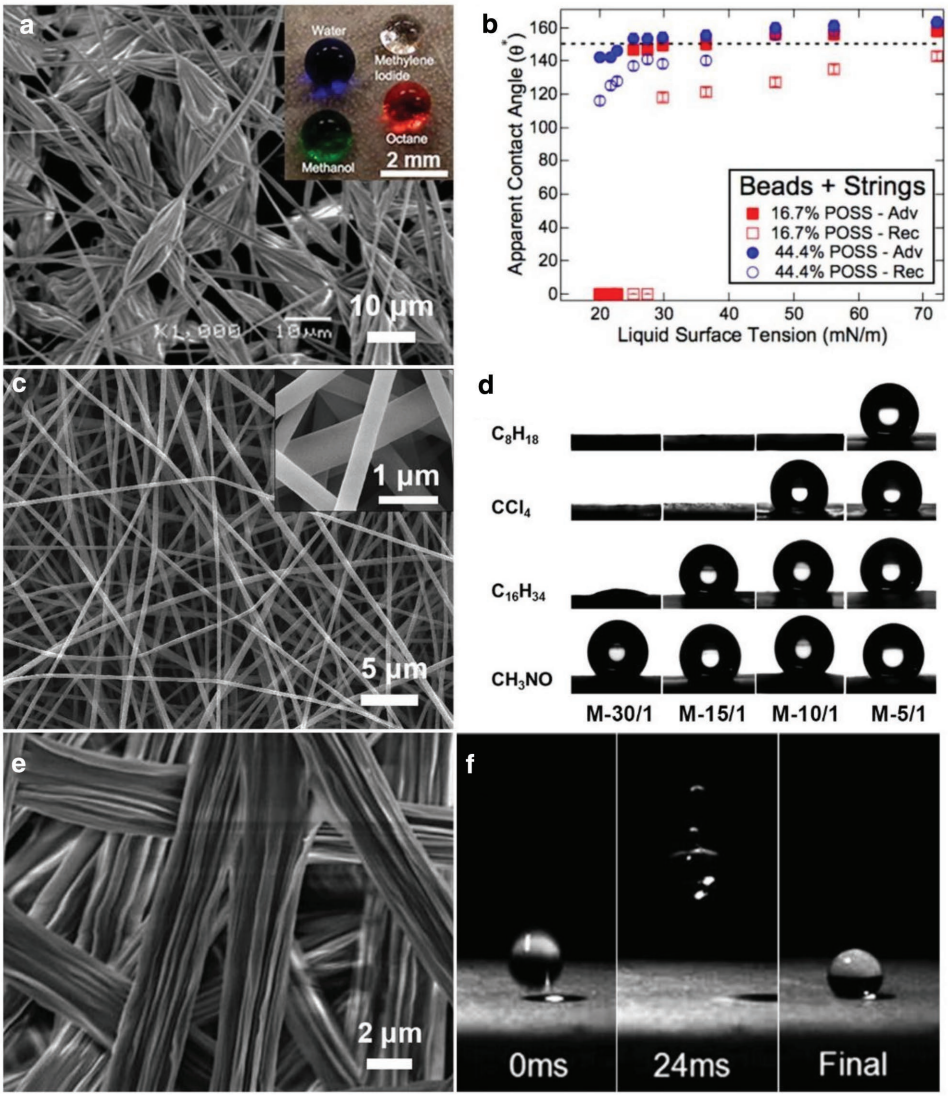

Figure 4. Electrospun superoleophobic surfaces a,b) Superoleophobic fluorodecyl POSS-PMMA beads-on-string fibers.[136] c,d) lyophobic tunable PVDF-HFP nanofibrous membranes.[144] e) A superamphiphobic PCL/Teflon surface f) Water droplets will bounce away from the fiber surface, exhibiting its lyophobic property.[145] Reproduced with permission.[136] Copyright 2008, Anish Tuteja et al., Published by National Academy of Sciences. Reproduced with permission.[144] Copyright 2016, Lanlan Hou et al., Published by Springer Nature. Reproduced with permission.[145] Copyright 2009, American Chemical Society.

electrospinning.[152] **Figure 5**a contains SEM image of TiO_2 fibers that were obtained using the sol–gel, electrospinning, and calcination. The TiO_2 fibers mat showed an ultrafast spreading property within only tens of milliseconds (Figure 5b). The micropores and nanochannels in the composite hierarchical structures lead to the ultrafast-spreading due to the multiscale 3D capillary effect. Recently, a fast-spreading superhydrophilic mat was obtained by electrospinning hydrophobic linear triblock copolymer styrene-b-ethylene-butylene-b-styrene (SEBS) blends with amphiphilic PEO–PPO–PEO (F127) molecule.[153] It formed a micellar structured F127/SEBS system with F127 homodisperse coated on the SEBS film surface when the content of F127 was 20 wt%, as indicated by X-ray photoelectron spectroscopy. The morphology of micellar structured F127/SEBS system led to a surface wettability change from hydrophobic to superhydrophilic (Figure 5c). Zhu et al. produced α-Fe_2O_3 nanofibers from electrospun poly(vinyl alcohol) (PVA)/ferrous acetate composite precursors.[157] The morphology and crystalline phase of α-Fe_2O_3 nanofibers could be controlled by the content of ferrous acetate and the calcination temperature. The rough surfaces of the α-Fe_2O_3 nanofibers contributed to the superhydrophilic property. Tijing et al. fabricated tourmaline (TM) nanoparticle-decorated polyurethane (PU) composite nanofibers with superhydrophilic and antibacterial properties by one-step electrospinning in Figure 5d.[154] The decoration of TM nanoparticles on the surfaces of fibers decreased water CA of the neat PU film from 125° down to 13°, as shown in Figure 5e. The introduction of TM nanoparticles as a kind of hydrophilic polar crystalline material is responsible for tuning the surface energy and the surface roughness of the

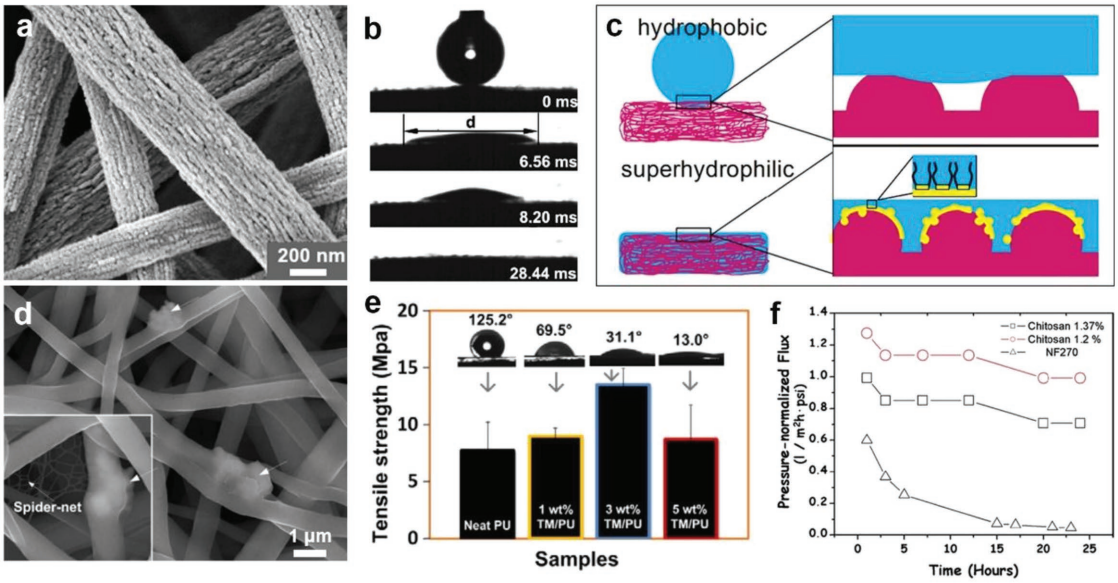

Figure 5. Electrospun superhydrophilic nanofibers. a,b) Ultra-fast water spreading on the superhydrophilic porous TiO_2 nanofibers mesh[152] c) Scheme of a water drop in contact with electrospun mats for the hydrophobic and superhydrophilic compositions.[153] d) tourmaline decorated PU electrospun nanofibrous with spider-net like morphology.[154] e) The wettability of the PU nanofibrous membrane changes from hydrophobic to hydrophilic with the increasing tourmaline content. f) enhancement of hydrophilic is benefit for increasing flux of separation membrane.[155] Reproduced with permission.[155] Copyright 2009, American Chemical Society. Reproduced with permission.[153] Copyright 2015, American Chemical Society. Reproduced with permission.[154] Copyright 2012, Elsevier. Reproduced with permission.[155] Copyright 2006, Elsevier.

composite films. On one hand, the TM particles improve the fiber hydrophilicity due to its hydrogen bonding with water molecules. On the other hand, the sub-nanofibers network structure also enhanced the hydrophilicity. The TM/PU composite mats with improved mechanical properties, superhydrophilic surfaces, and good antibacterial properties may have potential applications in the fields of antibacterial materials and water filtration. Lim and co-workers then reported a electrospun hydroxyapatite/nylon-6 (HAP/N6) biocomposite hydrophilic nanofiber film of easy controllable porosity.[158] In this work, the pristine hydrophobic N6 fibers can convert to superhydrophilic fibers at 10 wt% HAP particles. Hsiao and co-workers reported a high flux ultrafiltration membrane by electrospinning PAN scaffold combining with a thin top layer of hydrophilic chitosan coating.[155] The as-prepared three layered membranes exhibited much higher flux rate for water during 24 h compared with the commercial nanofiltration filter (Dow NF270) (Figure 5f).

4. Applications of Superwettability Electrospun Materials

In general, the development of new materials science goes through the stages of performance research and functional explorations. In the past two decades, the preparations of bioinspired superwetting materials have laid a solid foundation for the applications. As discussed in the previous sections, electrospun fibers are usually of large specific surface area, high porosity, excellent flexibility, and small interfiber pore size. The unique properties make the electrospinning materials play a significant role in ranges of selective liquid mixtures separation, water collection, unidirectional penetration, as well as smart controllable wettability materials and other fields. Herein, some applications of the electrospun fibers with superwettability are briefly discussed.

4.1. Oil/Water Separation

In the past ten years, superwettability electrospun materials with superhydrophobic and superoleophilic have proved to be a good candidate for selectively removing oil from water. Electrospun membranes are consisting of continuous, porous nonwoven micro/nanofibers with high surface area and well-designed superwettability properties that make them suitable for oil/water separation applications. In general, according to the way the oil is removed, the materials can be mainly divided into two categories: oil absorption materials and oil filtration materials.

4.1.1. Oil Absorption Nanofibers

The occurrence of pollution of oil spill accidents has brought great destruction to ecological environment due to its damaging impacts, which are usually of large area of pollution and tremendous amount of oil content.[159] In recent years, oil absorbing materials have drawn much attention because of their unique advantages in the rapid treatment for accidental marine oil spills.[160–165] Therefore, the oil absorption materials are requested to satisfy several conditions: i) large oil absorption amount, ii) high oil absorption speed, iii) cheap and easy preparation in large quantities. According to the three requirements of oil absorption materials, we have fabricated secondary pore structure superhydrophobic/superoleophilic PS film with macropores interleaved between the fibers, and micropores on the fibers surface generated

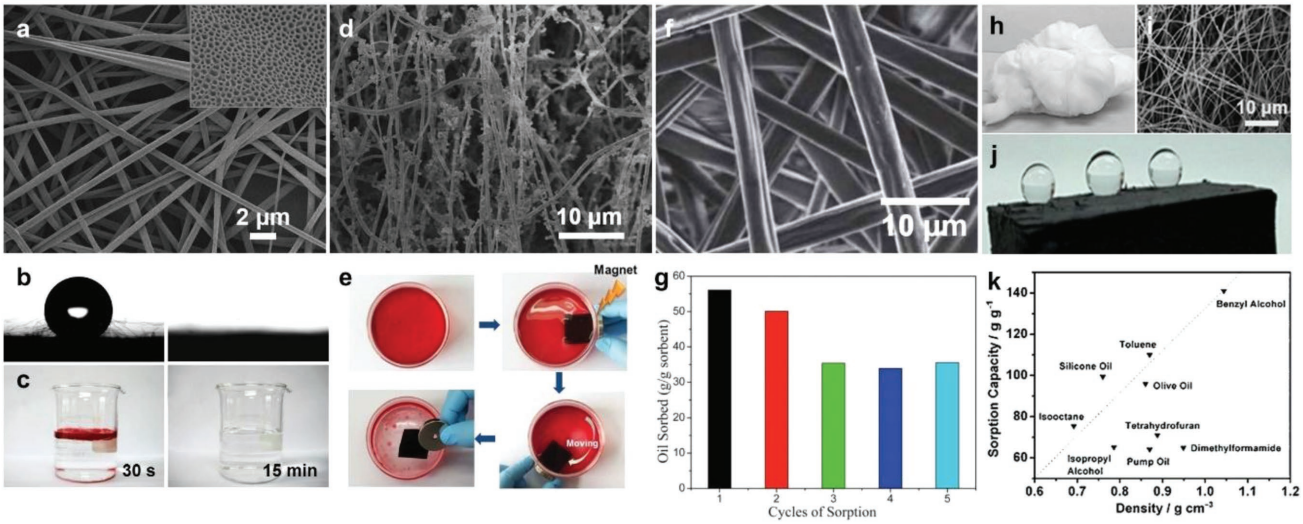

Figure 6. The electrospun micro/nanofibrous membranes for oil/water absorption separation. a) The porous PS fibrous film. Inset shows the microporous surface structure of fiber.[166] b) The PS fibrous film presents superhydrophobic (left) and superoleophilic (right) properties. c) Oil spill removal from water by porous PS fibrous film (oil dyed with oil red). d) magnetic Fe_3O_4 nanoparticles decorated nanofibrous membrane.[167] e) magnet-driven oil removal (oil dyed with oil red). f) PS-PU composite membranes.[168] g) The oil absorption ability of PS-PU membrane towards five cycles for motor oil. h,i) PAN-silica nanofibers sponge.[169] j) The carbon-silica sponge exhibited a superhydrophobic property. k) The absorption capacity of the sponge for oils and organic solvents of different density. Reproduced with permission.[166] Copyright 2012, American Chemical Society. Reproduced with permission.[167] Copyright 2015, Royal Society of Chemistry. Reproduced with permission.[168] Copyright 2013, Royal Society of Chemistry. Reproduced with permission.[169] Copyright 2015, Wiley-VCH.

by microphase separation (**Figure 6**a,b).[166] Compared with smooth fibers without porous structure, the as-prepared membranes presented higher oil absorption capacity. As in a mixture of motor oil and water of 1:10 (w/w), almost all of the oils were absorbed by the PS membrane within 15 min (Figure 6c). The two-tier porous structure of the electrospun PS nanofibers played an important role in improving oil absorption capacity and oil/water selectivity. The results showed that the oil absorption capacities of porous PS sorbent films toward diesel oil, silicon oil, peanut oil, and motor oil were ≈7.13, ≈81.40, ≈112.30, and ≈131.63 g g^{-1}, respectively. The weight of the adsorbed oil was even more than 100 times greater than that of the films themselves. Moreover, in view of the inconvenient collection of the material after oil absorption, we synthesized smart magnet driven fibrous films for remote oil removal recently. Magnetic Fe_3O_4 nanoparticles were easily anchored onto electrospun PVDF fibrous films (Figure 6d).[167] The as-prepared superhydrophobic/superoleophilic hierarchical structured membranes showed high oil absorption capacity after fluorination. Importantly, because of the magnetic controllability endowed by the Fe_3O_4 nanoparticles, the as-prepared fibrous films quickly adsorbed oil from the mixed solution, and the film then be moved in the direction of the magnetic field (Figure 6e). This work provides a new strategy for designing smart responsive oil removal materials, which would have broad applications in complex oil-polluted water treatment and oil spill clean-up. The coaxial electrospinning technique, with the PU and PS materials selected as the core/shell solution, has also been used to prepare a hydrophobic and oleophilic fibrous material, as shown in Figure 6f.[168] The as-prepared sorbent revealed high sorption capacities toward motor oil and sunflower seed oil up to 64.40 and 47.48 g g^{-1}, respectively. Figure 6g illustrates the oil absorption ability of the composite PS/PU core nanofibrous materials for five cycles, showing a decrease no more than 40% of its initial absorption ability. Sun and co-workers have prepared a carbon–silica sponge by electrospinning and carbonization PAN–silica into carbon–silica material.[169] Figure 6h,i revealed the photograph and SEM image of the origin PAN–silica nanofibers with fiber diameters ranging from 300 to 500 nm. The sponge after carbonization exhibited enhanced toughness and resistant to deformation. Silicone oil was then coated on the carbon–silica sponge to improve its hydrophobicity and exhibited a superhydrophobicity in Figure 6j. The obtained sponge exhibited an outstanding oil absorption capacity for a range of oils and organic solvents up to 65 to 140 times of their own weight in Figure 6k. These works indicated that electrospun superwettability nanofibers could serve as promising materials for efficient oil absorption.

As discussed above, most of current oil absorption materials are based on the superhydrophobic/superoleophilic property, which could selectively absorb oil from water. However, it is worth noting that these materials could not completely recover the absorbed oil from porous media because of the high oil affinity. The adhered oil residual in the pores decays the absorption of materials that make such materials only show best performance in first circle while dropping a lot in the following usage. According to the wetting theory, such superhydrophobic/superoleophilic material forms a gas/liquid/solid triple phase contact when it contacts to oil and water. Recently, we designed a unique underwater oleophilic but oil nonwetting surface in an oil/water/air/solid system.[170] That is based on an air superamiphiphobic low surface energy surface. If the surface is underwater, oil could spread on the surface but will not wet the surface. Take the nitroanisole oil as an example, the droplet on surface showed a superrepellent state with OCA of 161.5° ± 7.6° in air, however, an oleophilic state of 54.3° ± 5.1° but nonwettable underwater. In addition, the nitroanisole droplet can slip down

along the surface completely without residue. In that oil/water/air/solid system under water, these dense air pockets reside in the nanogrooves leading to a liquid/air interface on the solid surface. The decrease of system free energy, due to the replacement of high energy water/air interface by the low energy oil/air interface, plays a major role in lyophilic nonwettable Cassie state. The exploration of a nonwettable Cassie state provides a theoretical basis and guidance for designing new oil absorbing materials with good recyclability. We have designed such resuable oil collection materials by a 3D network organosilane surface with excellent thermal and chemical stabilities.[171] Despite notable progresses have been made for highly efficient oil absorption, the challenges on how to fabricate materials with both high absorption and high recyclability, as well as how to absorb high viscous oils or complex oil contaminates still need to be explored.

4.1.2. Oil/Water Filtration Separation

Conventional oil/water mixtures separation methods, such as distillation, extraction, ultrasonic, electrochemical treatment, and gravity separation, cannot meet the requirements of separation efficiency.[165,172,173] Meanwhile, it is limited by the disadvantages of large energy consumption, secondary pollution, and unrecyclability. The scientists found the superwetting materials are very attractive for efficient oil/water separation.[174–179] The electrospun nanofibers membranes have been proven a promising choice for oil/water filtration separation. Wang et al. reported the separation of oil/water mixtures by electrospun bead-on-string structured superhydrophobic thermoplastic polyurethane (TPU) mats.[184] After treating it with hydrophobic nanosilica, the initial TPU electrospun film became superhydrophobic, so that it could be used for separating oil and water mixtures. Yoon and co-workers prepared electrospun PS nanofiber membranes with superhydrophobicity and superoleophilicity for separation of water and low viscosity oil.[185] The combination of low-free-energy PS nanofibers with the 3D network structures induced by electrospinning enhanced the dewetting of water, while keeping the intrinsic wettability by oil. The PS nanofiber membranes easily separated low-viscosity oil from water and also exhibited excellent superhydrophobicity even after many cycles. Recently, Ding and co-workers presented some superhydrophobic and superoleophilic nanofibrous membranes prepared by facile electrospinning technology combining with in situ polymerization method, exhibiting good oil/water separation performance.[186] By employing fluorinated polybenzoxazine incorporated with SiO_2 nanoparticles, the pristine hydrophilic cellulose acetate nanofibrous membranes were endowed with superhydrophobicity and superoleophilicity.[180] **Figure 7**a illustrated the fluorinated cellulose acetate membranes with the high roughness exhibiting the superhydrophobicity with a WCA of 161°. The wettability of the membranes could be manipulated by tuning the surface composition and the hierarchical structures. As Figure 7b revealed, the WCAs on the modified electrospun cellulose acetate nanofibers increased with the concentration of synthesized bifunctional fluorinated benzoxazine (BAF-tfa). Meanwhile, it demonstrated the selective and efficient separation of oil/water mixtures by the as-prepared membranes.

Besides direct electrospun route, some post-treatment methods are employed to fabricate superwettability membrane combined with electrospinning. Sun and co-workers fabricated a silica–carbon mat by electrospunning of the blended PAN and silica precursor solution to generate nanofibers, and then

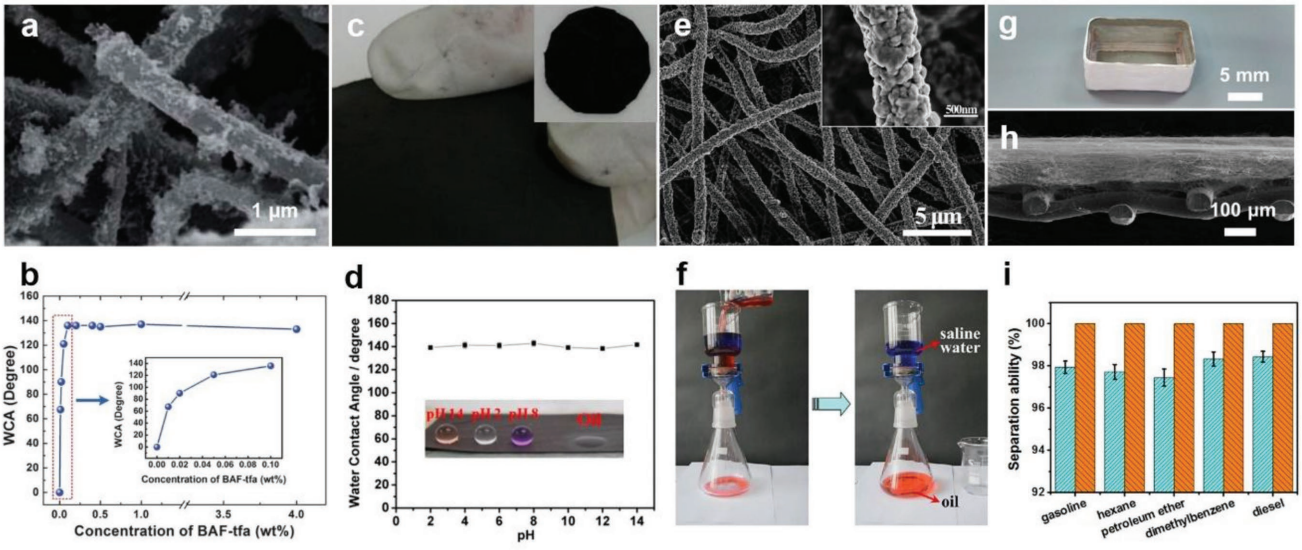

Figure 7. Nanofibrous oil-water filtration membranes. a) The superhydrophobic SiO_2 nanoparticles modified cellulose acetate nanofibrous membranes.[180] b) The variation of the WCAs of the modified cellulose acetate nanofibrous membranes with different concentrations of bifunctional fluorinated benzoxazine. c,d) The flexible superhydrophobic carbon-silica membrane with wide pH stability.[181] e,f) Oil-water separation using Ag doped APAN nanofibrous membranes.[182] g,h) The oil collection box made from stainless steel supported PVDF-HFP nanofibrous membrane.[183] i) The separation abilities of the integrated oil collection box towards kinds of oil/water mixtures. Reproduced with permission.[180] Copyright 2012, Royal Society of Chemistry. Reproduced with permission.[181] Copyright 2014, American Chemical Society. Reproduced with permission.[182] Copyright 2014, American Chemical Society. Reproduced with permission.[183] Copyright 2017, Shanshan Qiu et al., Published by Royal Society of Chemistry.

subsequently the carbonization treatment.[181] Figure 7c demonstrates the nanofibrous mat showing excellent flexibility, the inset illustrated that the carbon–silica membrane can be cut into various shapes easily. In addition, the silica–carbon composite membrane possesses excellent environmental stability even exposed to aqueous solutions with a broad pH ranges from 2 to 14 (Figure 7d). The stable superhydrophobicity and porosity enable the silica–carbon membrane effectively separate oil from water. Wang and co-workers prepared Ag nanoclusters coated electrospinning amination polyacrylonitrile (APAN) nanofibers scaffold (Figure 7e). After decoration by n-hexadecyl mercaptan, the fibers exhibited superhydrophobicity and superoleophilicity.[182] The density of Ag nanocluster increased with the increasing of electroless plating time. In Figure 7f, the oil can be quickly separated from the oil and NaCl solution mixture by the membrane. Aiming at the floating oil collection, we designed an oil collection boat, which is made through assembling PVDF-HFP nanofibers onto stainless steel framework (Figure 7g,h).[183] The PVDF-HFP is hydrophobicity to water but superoleophilicity to various low surface tension oils including gasoline, hexane, petroleum ether, dimethylbenzene, and diesel oil. The micropores on the wall of the boat allowed oil penetration but prevented water infiltration. The floating oil could be gathered into the boat and be easily collected. Figure 7i demonstrates the oil/water separation ability for oil/water separation efficiency (blue column) and the purity of the collected oil (yellow column). The purities of the collected oils are higher than 99.99%. As introduced above, the electrospun membranes have become a prominent material for oil-polluted water treatment.

4.2. Emulsion Separation

In general, oil/water mixtures usually exist in three forms, i.e., free oil with droplets diameter larger than 150 μm, dispersed oil of 20–150 μm, and the emulsified oil with dispersed phase less than 20 μm. Besides the free oil droplets, the emulsified oil/water mixtures, especially surfactant-stabilized emulsions, are more difficult to be separated, which has become a worldwide challenge. The membrane separation has been studied as the most effective way to remove the emulsified oil from oily wastewater with the emergences of microfiltration, ultrafiltration, and nanofiltration membranes, as well as their achievements.[187–190] In recent years, superoleophobic/superhydrophilic and superhydrophobic/superoleophilic porous materials have been explored for oil/water and water/oil emulsions separation. Previous research confirmed that "wetting effect" and "sieve effect" are two key factors in emulsion separation.[50,191,192] The porous electrospun materials as the filtration fibrous membranes with superwettability meet exactly these two requirements, which have thereby became a promising choice for fabricating emulsion separation membranes.

The hydrothermal post-treatment combined with electrospinning technology is a common approach to fabricate superwettability emulsion separation membranes. Recently, we have proposed a multilevel structure pine-branch-like TiO_2 membrane through electrospinning and subsequently calcination (**Figure 8**a).[193] The pine-branch-like secondary structure on every TiO_2 fiber effectively reduces the size of the pores, which is important for emulsion separation. The as-obtained TiO_2 membrane can be applied in oil-in-water emulsions separation

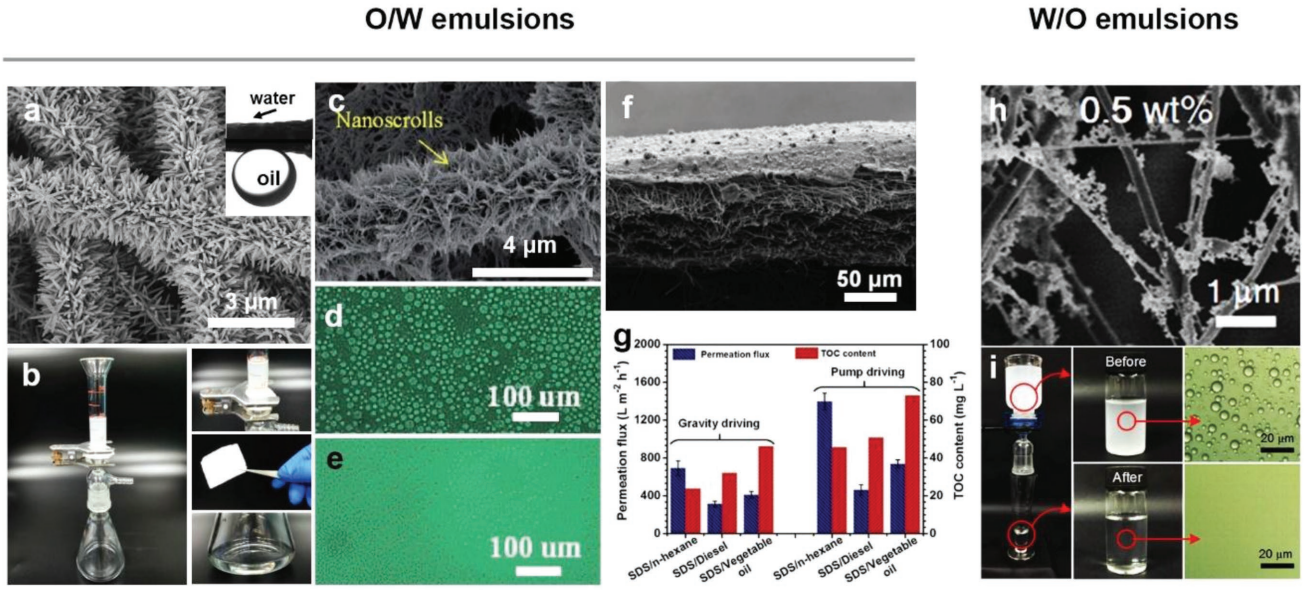

Figure 8. Electrospun nanofibrous membranes for high efficient O/W and W/O emulsions separation. a) Pine-branch-like structured electrospun TiO_2 fibrous membrane.[193] b) gravity-driven separation of gasoline-in-water emulsion using branch TiO_2 fibrous membranes. c) The modified sponges with hierarchical structured SiO_2 nanofibers.[194] d,e) The optical microscopy images of emulsion and its filtrate. There is no oil droplet was found in the filtrate that proved the effective separation. f) PAN nanofibrous membranes coated with a rough PAN skin layer surface by electrospinning and electrospraying.[195] g) The permeation flux and the total organic carbon contents after separation of various SDS surfactant stabilized O/W emulsions under gravity and the driving of different pressures. h) PAN/SiO_2 aerogels.[196] i) The optical micrographs of the W/O emulsion before and after separation. Reproduced with permission.[193] Copyright 2017, Royal Society of Chemistry. Reproduced with permission.[194] Copyright 2017, Wiley-VCH. Reproduced with permission.[195] Copyright 2018, Wiley-VCH. Reproduced with permission.[196] Copyright 2015, American Chemical Society.

even in various high corrosive acidic (pH < 0), basic (pH > 14), and salty media. Figure 8b gives an illustration of the separation setup. The calculated separation efficiencies toward different oils are all exceeding of 99%. Similarly, Du and co-workers fabricated an ultrasmall pore size membrane through introducing of layered double hydroxides and SiO_2 electrospun nanofibers into the robust porous poly(melamine formaldehyde) (PMF) sponges frame.[194] The average pore size of the modified PMF sponges can be varied by the SiO_2 nanofibers concentration. Figure 8c reveals the hierarchical structures of the SiO_2 nanofibers. Combining the superhydrophilic property and suitable pore size, the sponges can be applied in effective separation of layered oil/water mixtures, surfactantfree or surfactantstabilized oil/water emulsions driven by gravity only. Figure 8d,e illustrates the microscopy images of emulsion before and after separation. Besides, they have designed a series of sponges with controlled pore sizes and the ratio of pore size/thickness, which allow the obtained sponges to be effectively applied in broad ranges. Recently, Ding and co-workers prepared a flexible, thermally stable, and hierarchical porous silica nanofibrous membranes.[197] The membranes show superhydrophilicity and underwater superoleophobicity, which can be used for O/W emulsions separation. With increasing SiO_2 nanoparticle concentration, the mean pore size slightly decreased because of the SiO_2 nanoparticles positioned on the surfaces of the nanofibers rather than in the voids of the nanofibers. The separation performances of the membranes were obviously improved by the hierarchical porous structure, which was induced by the synergistic effects of mesoporosity and macroporosity. Accordingly, the silica nanofibrous membranes could effectively separate microsize surfactant-stabilized oil/water emulsions driven by gravity with high separation efficiency. They further reported a lotus-leaf-like micro/nanostructured surface with a skin layer by electrospraying and electrospinning simultaneously in Figure 8f.[195] The membrane possesses superhydrophilic and underwater superoleophobic properties with the underwater OCA of 153°. In addition, the ultrathin skin layer with high porosity can effectively intercept tiny oil droplets while allowing the water permeation in a high flux. Figure 8g shows the permeation flux and the total organic carbon content for three kinds of surfactant stabilized emulsions that include sodium dodecyl sulfate (SDS)/n-hexane/H_2O, SDS/diesel/H_2O, and SDS/vegetable oil/H_2O.

In addition to oil/water emulsions, water/oil emulsion is another form and also widely studied. As we knew, the products of electrospinning are usually nonwoven fabrics of weak contact rather than strong chemical bonds between the fibers. Therefore, it involves an issue of the materials' life and performance cyclic stability. Ding and co-workers have reported advanced process in superelasticity aerogels by electrospinning and freeze-shaping techniques, which can be used for highly efficient water/oil emulsion separation with high flux (Figure 8h,i).[196,198] The obtained elastic bulk aerogels can be generated into various desirable shapes in a large scale. At present, the method to prepare materials used for emulsion separation is mostly achieved by reducing the pore size. Despite the achievements, however, some problems such as the membrane fouling and recycling performances as well as a trade-off between the flux and separation efficiency are still obstacles to be overcome.

4.3. Organic Liquid Separation

Multiple-phase organic liquid separation is currently an important issue, and closely related to the resource recycling, complex chemical products separation, and environmental protection. Most of processes of petrochemical industry, food, medical, textile printing, as well as the daily life all the time discharge large amount of oily liquid. Without being treated, it will bring great environmental pollution and resources waste. Thus, it is essential and significant to designing and fabricating materials in separation of mixed liquid products to avoid the wasting and polluting. Very recently, separation of immiscible organic liquid mixtures has been achieved by the liquids wettability difference on the materials. Based on that, the liquid mixtures can be separated on the membranes that exhibit superlyophobicity for higher surface tension liquid while superlyophilicity for lower surface tension liquid.[199,200]

The achieving of organic solvents separation, in fact, is an issue that ensures the two mixed liquids exhibiting different wetting behavior on the separation membrane. Recently, Jiang and co-workers developed a general strategy to separate immiscible organic liquids by manipulating the surface tensions of nanofibrous membranes. The membranes were fabricated by electrospinning, calcination, and surface modification.[201] **Figure 9**a is morphology of the membranes indicating the uniform TiO_2 fibers with multilayer networks and random pores. The superlyophobic sample with different surface tensions can be obtained by modification of different silanes. As shown in Figure 9b, the fibrous membranes show increasing lyophobicity with the increase of −CF chain. Thus, the surface energy of membrane can be controlled between the surface tension of two liquids that is $\gamma_{sv(A)} > \gamma_{sv} > \gamma_{sv(B)}$, which can achieve separation for different organic liquids in Figure 9c. For example, the fibrous membrane exhibits superlyophobicity for formamide and superlyophilicity for tetrachloromethane (CCl_4), then the mixture of formamide and CCl_4 could be separated due to the different wettabilities of the membranes. This work opens a field for designing separation membranes not only for oil/water separation, but also for organic liquids separation. However, problems are exposed that the surface energy is discontinuously controlled by limited range of fluorosilane species, in addition, the intrinsic brittleness of inorganic materials limits the applications of the membranes. Therefore, we designed a flexible PVDF-HFP doped 1H, 1H, 2H, 2H-perfluorodecyltrimethoxysilane (PFDTMS) nanofibrous nonwoven membrane with precisely tunable wettability that could be used in multiphase organic liquids separation.[144] By controlling the content of PFDTMS, the surface free energy of the membrane could be tuned falling in between the surface tension of two organic liquids. Thus, aimed at different multiphase liquid systems, the fibrous membranes could intercept the relatively high surface tension liquid and allow passing through of low surface tension liquid (Figure 9d). Figure 9e,f shows that formamide (blue) and CCl_4 (red), ethylene glycol (green), and dimethylbenzene (red) could be well separated by the membranes. The membranes show the high separation efficiency and durable cycle stability for organic liquids separation. Besides the modification of membrane surfaces by the low surface energy fluorosilane, a stable liquid-infusion-interface is also another smart strategy for nonwetting surfaces.[149] Inspired by the slippery surface of Nepenthes pitcher plant, well-designed infused flexible SiO_2–

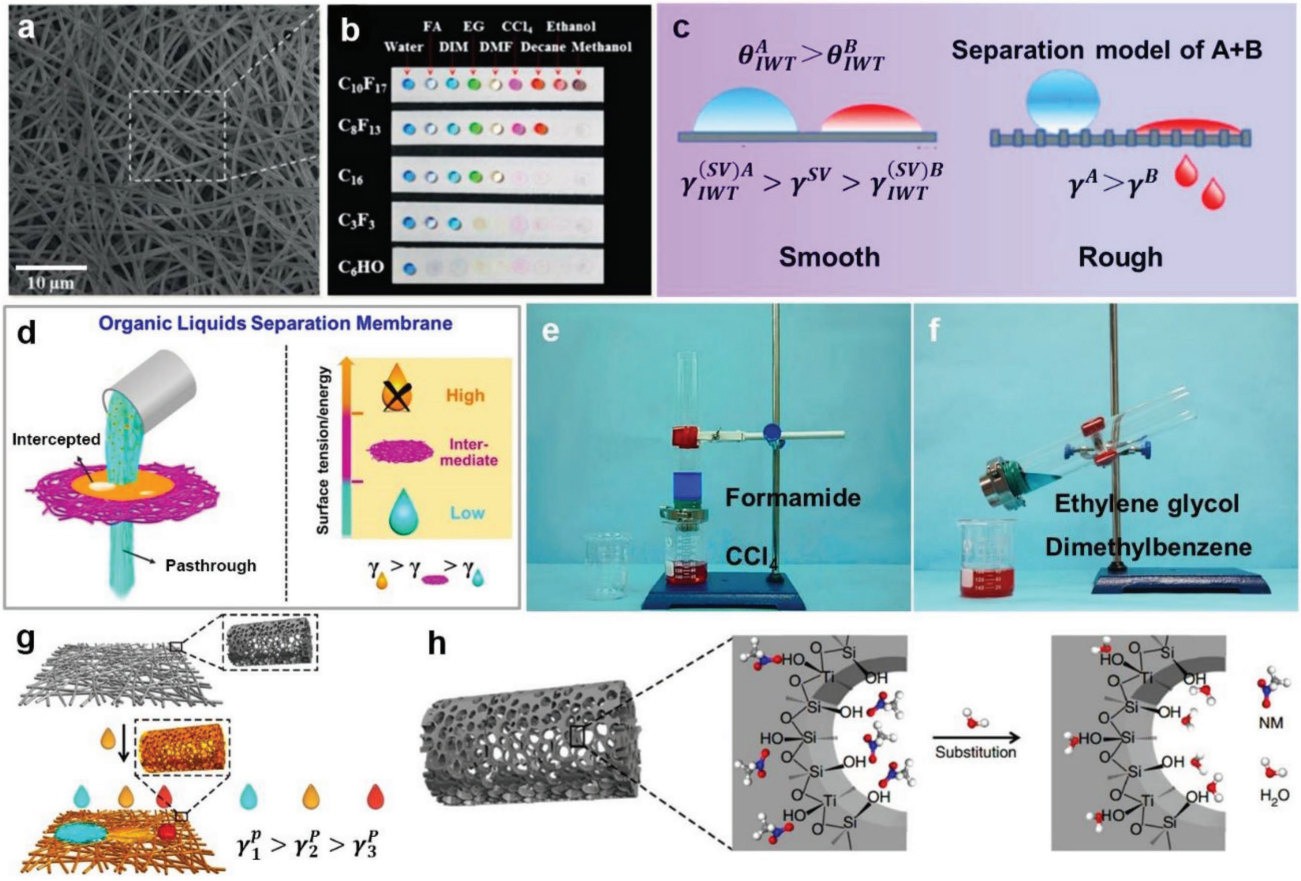

Figure 9. Separations of multiphase organic liquids mixtures by electrospinning membranes with controllable wettability. a) Nanofibrous TiO_2 membrane of low surface energy.[201] b) The liquid repellent abilities of various fluorosilane modified TiO_2 membranes towards liquids with different surface tension. c) The separation model and result of liquid mixtures, which depend on the different wettability of liquid A and liquid B on the membrane. d) Scheme of multiphase organic separation.[144] The separation results of e) formamide and CCl_4 mixtures and f) ethylene glycol and dimethylbenzene mixtures. g,h) The mechanism of multiphase liquid separation by liquid infused membrane.[202] Reproduced with permission.[201] Copyright 2015, Wiley-VCH. Reproduced with permission.[144] Copyright 2016, Lanlan Hou et al., Published by Springer Nature. Reproduced with permission.[202] Copyright 2017, Yang Wang et al., Published by Springer Nature.

TiO_2 composite porous nanofibrous membranes (STPNMS) were prepared with tunable liquid repellent ability.[202] In this system, the polar to polar interaction is predominant to the membrane's surface energy. The wetting behavior of the superamphiphilic STPNMS can be regulated by infusing a high polar surface energy liquid that to form a relatively stable liquid-infusion-interface, repelling the immiscible liquid of lower polar surface energy (Figure 9g). As a result, the liquid with a much higher polar surface energy than the infused liquid can selectively penetrate the STPNMs. Moreover, the infused liquid can be substituted by an immiscible liquid with higher polar surface tension directly as in Figure 9h, facilitating the successive separation of multiphase liquids. These membranes are expected to become competitive candidate for complex organic chemical products separation, resource recycling, as well as environmental protection.

4.4. Water Collection

In nature, many of the biological surfaces, for instance, butterfly wings, rice leaves, and bird feathers, possess unique wettability owing to their special structural features at the micro/nano scales.[203] Comparing to 2D surfaces, 1D materials are attracting more and more attentions recently due to their applications in water condensation and harvesting, liquid transportation, and microfluidic devices. Driving of liquid drops in a directional manner is of great interest. For example, a spider's web decorated with shiny water droplets is usually a beautiful sight in the early morning. Spider silks have a unique ability to deform in the presence of moisture and rebuilt periodic spindle-knots by wetting. The tiny water droplets can self-move from the joints to the spindle-knot structures (**Figure 10**a,b).[15] The driving force of this motion is Laplace pressure that is generated by the gradient between the spindle-knots and the joints. Thus, many researchers are devoted to design such fibers that could mimic the beaded structure and water collection performance of spider silk.[204–207] As demonstrated in Section 2, the ultimate shape of electrospun fibers is decided by the competition of viscoelasticity and Rayleigh instability. If lower viscous solutions are used, the Rayleigh instability will prevail and result in spindle shaped fibers. In most cases, such beaded fibers give undesirable results because of their irregular structure. Every coin has two sides, however, it can

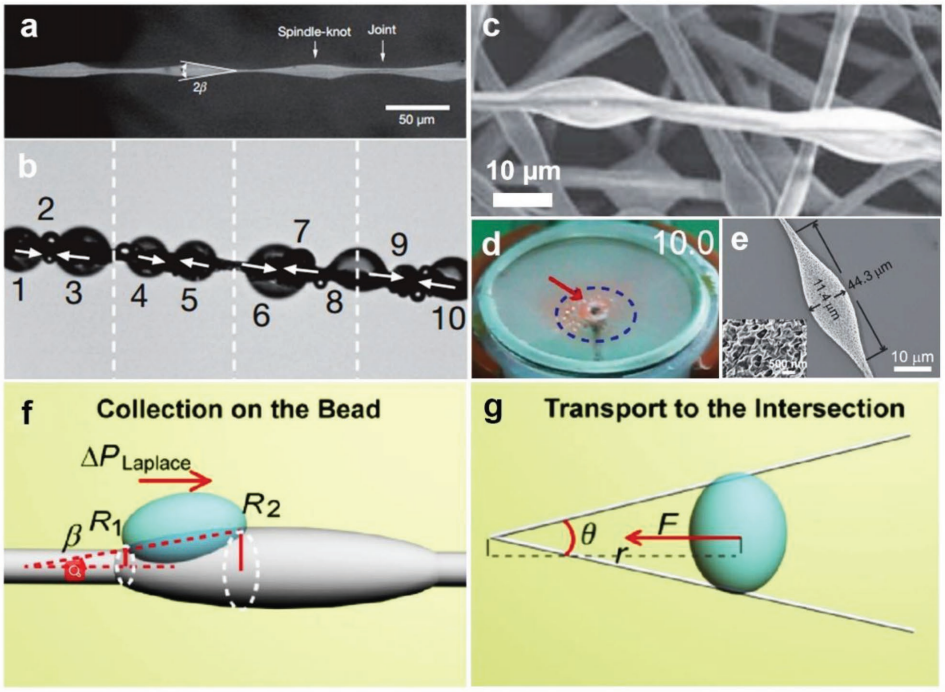

Figure 10. Nature and artificial electrospun spider silks for water collections. a) A spider silk with periodic spindle-knots linked with slender joints, b) water collection on a spider silk.[15] c) The bead-on-string heterostructured fibers by electrospinning.[207] d,e) radial patterned water collector composed of spindle electrospun fibers.[208] f) Mechanism of water directionally moves from smaller radius to large radius. g) The liquid collection mechanism on fibers system. Reproduced with permission.[15] Copyright 2010, Springer Nature. Reproduced with permission.[207] Copyright 2011, Wiley-VCH. Reproduced with permission.[208] Copyright 2016, Wiley-VCH.

be seen that such periodic spindle fiber is very similar to natural spider silks. Therefore, electrospinning has been applied to fabricate spider-silk-like bead-on-string fibers for water collection.[207] For example, the inner PS solution with high viscosity and the outer PEG solution with low viscosity were used to coaxial electrospinning, then PS/PEG core–shell bead-on-string heterostructured fibers with different chemical compositions could be prepared (Figure 10c). We also employed the Rayleigh instability effect to generate spindle-knots on fibers through coaxial electrospinning.[64] A concentrated PS solution and a low viscosity PMMA solution worked as the inner and outer fluids. When a high-voltage electrical field was applied, the viscous PS solution was stretched into fibers, whereas the dilute PMMA solution flowed out and adhered to the PS fiber surface. Then, the PMMA liquid film formed a series of liquid drops, which solidified into periodic spindle-knots on the PS fibers. The flow rates and the concentrations of the two solutions affect the morphology of the fibers. When the as-prepared spindle-knot fiber was set in a high relative humidity environment, tiny water drops condensed on the fiber, moved toward the spindle-knots, and became integrated with each other under the Laplace pressure. It thereby achieved water collection purpose. Besides investigation of water collecting behavior on single fiber, Jiang and co-workers fabricated a novel radiate distributed beaded fibers, as shown in Figure 10d,e.[208] As illustrated in Figure 10f, on one hand, this gradient of the surface-free energy of single fiber produces a driving force for condensed fog droplets directionally transporting to the beads under the Laplace pressure. On the other hand, the adjacent fibers with wedge-angle also provide Laplace pressure further driving the tiny droplet moving toward cross point of two fibers (Figure 10g). As a result, the droplets from all directions were effectively collected at centre of collector and thereby achieved high efficiency water collection. These results demonstrate the simplicity and efficiency of electrospinning method to generate spider-silk-like fibers for water collections.

4.5. Unidirectional Liquid Penetration

As the name with inspiration from the two-faced Roman god Janus, scientists have named the membrane with opposing property at an interface of Janus membrane, which can bring anisotropic properties and special applications.[209–214] Cho and co-workers fabricated a bicomposite PAN film with superhydrophobicity on one side and superhydrophilicity on the other side (**Figure 11**a,b).[215] Similarly, Lin and co-workers recently designed directional oil-transport membranes, which consist of a layer of superhydrophobic/oleophilic nanofibers (PVDF-HFP) and a layer of superamphiphobic nanofibers (PVDF-HFP/POSS, PVDF-HFP nanofibers with fluorinated decyl polyhedral oligomeric silsesquioxane and fluorinated alkyl silane).[216] As Figure 11c shown, the PVDF-HFP layer reveals superoleophilic ability toward liquid with surface tension below 34.0 mN m^{-1}, and the PVDF-HFP/POSS layer exhibits an ultraoleophobic capacity for liquid surface tension above 23.8 mN m^{-1}. Therefore, the membrane displays unidirectional penetration only for liquid with surface tension in the range of 23.8–34.0 mN m^{-1}. Figure 11d,e demonstrates that the diesel be blocked on the

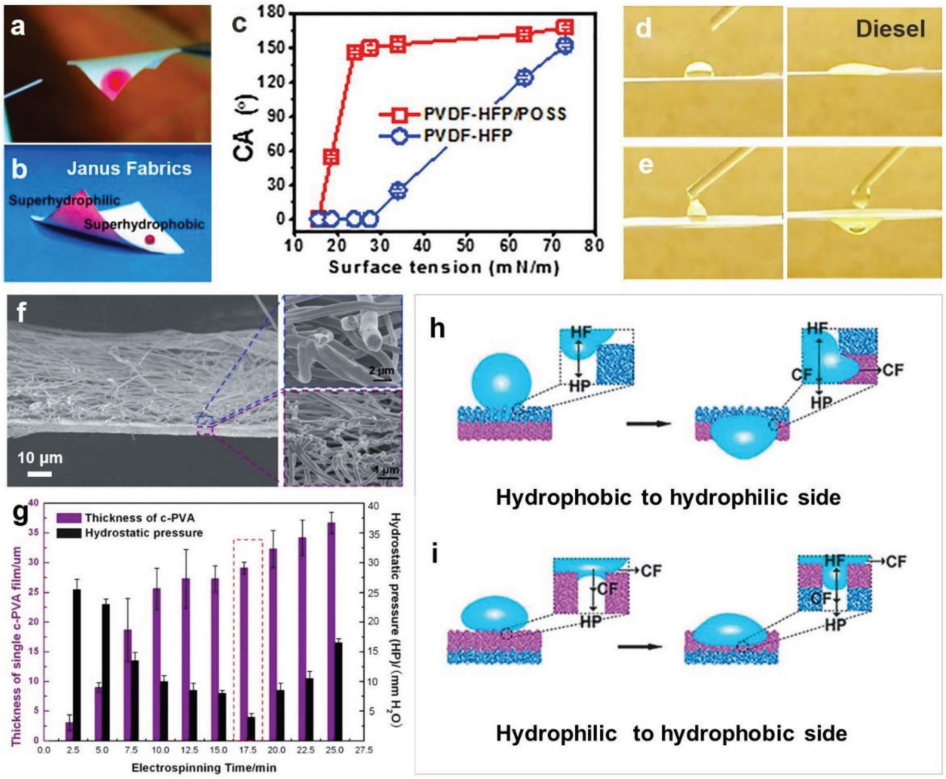

Figure 11. The liquid unidirectional penetration on the asymmetric wettability gradient membranes. a,b) Biphasic Janus fabric exhibited the superhydrophilic and superhydrophobic on its two sides.[215] c) CAs of water and various oils with different surface tension on the PVDF-HFP and PVDF-HFP/POSS membrane surfaces.[216] d,e) The unidirectional penetration of diesel drops on different sides of a dual-layer nanofiber membrane. f) Dual-layer PU/c-PVA composite fibrous film and the magnified sections of PU layer and c-PVA layer.[219] g) The hydrostatic pressure shows a firstly decrease and then increasing trend with the increase of c-PVA membrane thickness. h,i) The mechanism explanations of water behaviors on the two sides of the PU/c-PVA membrane. Reproduced with permission.[215] Copyright 2010, American Chemical Society. Reproduced with permission.[216] Copyright 2015, Wiley-VCH. Reproduced with permission.[219] Copyright 2012, Royal Society of Chemistry.

PVDF-HFP side, while penetrating from a PVDF-HFP/POSS to PVDF-HFP direction. Hence, this research can be applied in smart textures and flow control devices.[217,218]

Recently, we designed a "water diode" film with heterogeneous wettability in different directions by a facile electrospinning technique.[219] The composite film was composed of a fibrous hydrophobic PU film and a hydrophilic glutaraldehyde cross-linked PVA (c-PVA) film (Figure 11f). Taking advantage of the hydrophobic–hydrophilic wettability difference, water can spontaneously penetrate from the hydrophobic to hydrophilic direction, while be intercepted on the opposite direction. The performance of unidirectional water penetration is dominated by the thickness of both the hydrophobic fibrous film and the hydrophilic film. For the hydrophobic PU layer, it provides a resistance force for liquid to pass through, therefore the water penetration pressure increased with increasing PU thickness. For the hydrophilic c-PVA layer, however, water pressure first showed a decrease, and then increase trend with the c-PVA layer thickness increase (Figure 11g). It is because in this system, the capillary force from the hydrophilic layer provides a positive force to promote water penetrating through. Meanwhile, it generates a resistance for water duo to the long channel length. With the thickness increases, the latter effect becomes more predominant. As the mechanism in Figure 11h expressed, when water dropped on the PU side, it was forced by two opposite forces, that are hydrophobic force and hydrostatic pressure. The increase of hydrostatic pressure facilitates the water cross the PU thickness and reach the c-PVA membrane, then the capillary force together with the hydrostatic pressure help water penetration. When the water was dropped on c-PVA layer, the water spread on the nanofibrous layer due to the capillary force. In this case, when the water contacts with the interface of c-PVA and PU layer, the spreading water cannot provide enough hydrostatic pressure to overcome the hydrophobic force. As a result, water was blocked on the Janus membrane in hydrophilic to hydrophobic direction (Figure 11i). The wetting difference and appropriate film thickness are two dominant factors in guiding liquid unidirectional penetration. This kind of fabric will play a role in future applications for smart textile and liquid manipulation.

4.6. Smart Responsive Surfaces

Smart responsive materials have exhibited great concerns for their well response in environment, such as temperature, light, pH, and ionic strength.[220–223] The surface wetting behavior of stimulus-sensitive materials can be varied by changing the surface conformation.[224–227] The electrospinning has emerged

as a very attractive method in fabricating smart response wettability surfaces.

4.6.1. Thermoresponsive Surfaces

We have fabricated thermally responsive poly(N-isopropylacrylamide) (PNIPAAm)/PS composite films by the electrospinning technique.[228] PNIPAAm is a thermally responsive polymer of hydrophilicity below the low critical solution temperature (LCST, ≈32 °C) and hydrophobicity above the LCST due to the chains collapsed conformation. The wettability of the PS/PNIPAAm surface could change between superhydrophilicity and superhydrophobicity in the temperature range from 20 to 50 °C at a proper proportion. (**Figure 12**a,b). The combination of the stimulus-responsive polymer with the hierarchical micro/nanostructures creates the unique superwetting surface. Similarly, Gu et al. also prepared thermoresponsive PNIPAAm/PLLA nanofibrous films by electrospinning.[229] Kingshott and co-workers fabricated self-assembled core–sheath nanofibers with PCL as the core and thermoresponsive PNIPAAm as the sheath by single-spinneret electrospinning.[230] The wettability of the mats displayed evident changes from hydrophilicity to hydrophobicity when the temperature changed from 20 to 40 °C. Due to the versatility of the electrospinning method, it could be expected to produce other smart controllable wettability surfaces.

4.6.2. Photoresponsive Surfaces

Chen and Besenbacher fabricated a photoresponsive film with controllable wettability properties.[231] The nanofibers were prepared from electrospun biodegradable PCL modified by light-responsive azobenzene. Upon UV irradiation, the surface turns from hydrophobic to hydrophilic duo to the changes in dipole moment and surface free energy. The reversible light-responsive wettability changes resulted not only from the azobenzene surface functionalization, but also from the roughness supplied by the electrospun micro/nanoscale hierarchical structures. Recently, Yoon and co-workers developed a wettability switchable surface from superhydrophobic to hydrophilic.[232] The nanocomposite membranes were prepared by electrospinning hydrophobic PS nanofibers and electrospraying of hydrophilic TiO_2 nanoparticles. The surface morphology of the mats could be controlled by the electrical conductivity of the electrospinning solution (Figure 12c). The water CA of PS–TiO_2 nanocomposite film can dramatically reduce from 140° ± 3° to 26° ± 2° after exposure to UV irradiation (Figure 12d). Coincidentally, Xin and co-workers also designed UV light responsive TiO_2 doped PVDF materials by electrospinning, which can be used to control smart oil/water separation.[233] The as-prepared beads-on-string structured TiO_2/PVDF composites materials exhibited reversible switchable superhydrophobic/superoleophilic or superhydrophilic/underwater superoleophobic wettability upon heating treatment or UV irradiation (Figure 12e,f).

4.6.3. Other Responsive Surfaces

Recently, Yuan and co-workers developed smart nanostructured electrospun polymer mats with switchable oil/water wettability using CO_2 as the trigger.[234] The poly(N,N-diethylaminoethyl methacrylate) (PMMA-co-PDEAEMA) mats were fabricated by a method based on the combination of polymerization reactions

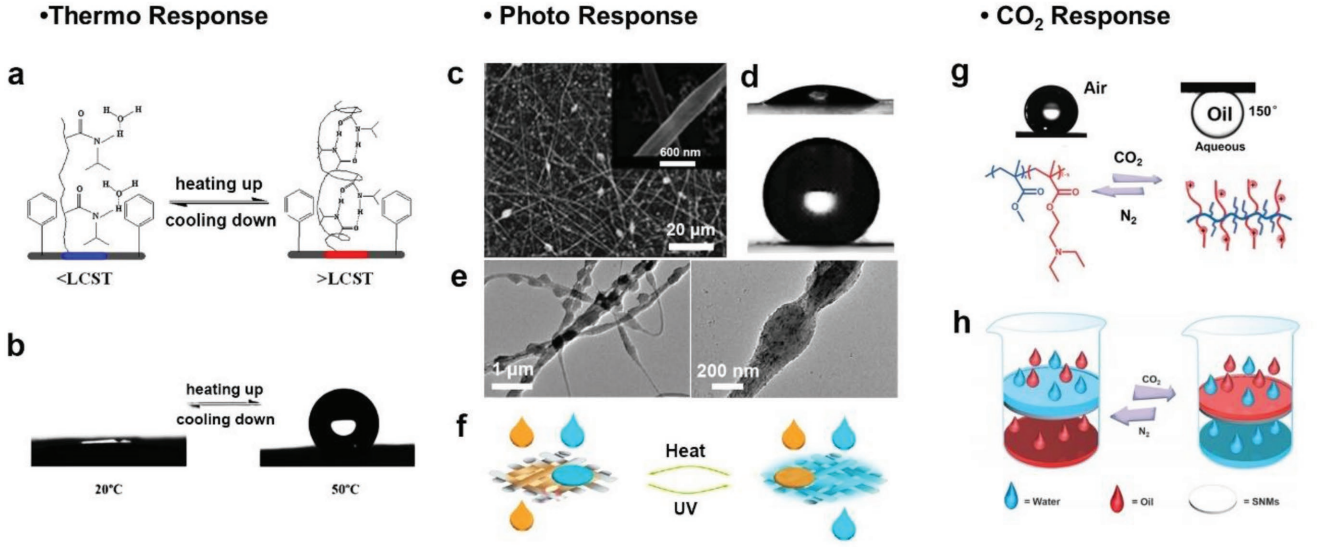

Figure 12. Smart responsive surfaces. a) The response mechanism of the thermally-responsive wettability of the composite film.[228] b) PNIPAAm/PS composite film show thermoresponsive switchable wettability properties. c,d) The water-droplet on the PS–TiO_2 nanocomposite mat before and after UV irradiation membrane via electrospinning and electrospray.[232] e) TiO_2 doped PVDF nanofibers.[233] f) PVDF/TiO_2 nanofibers show switchable superhydrophobic/superoleophilic or superhydrophilic/underwater superoleophobic wettability upon heating treatment or UV irradiation. g,h) CO_2-triggered oil/water wettability changes between hydrophobicity/oleophilicity and hydrophilicity/oleophobicity and application in oil/water on-off switch.[234] Reproduced with permission.[228] Copyright 2008, Wiley-VCH. Reproduced with permission.[232] Copyright 2013, Wiley-VCH. Reproduced with permission.[233] Copyright 2016, Wiley-VCH. Reproduced with permission.[234] Copyright 2015, Wiley-VCH.

and electrospinning. The smart mat exhibited a significant transition from hydrophobicity to hydrophilicity when exposed to CO_2 (Figure 12g). This obvious wettability transition could be explained by the protonation and deprotonation effects of amine groups in PDEAEMA. Meanwhile, the wettability of the film could return to the hydrophobic state after exposure to bubbling N_2. In an aqueous medium, the oil (hexane) wettability was changed from 36° to 150° after exposure to bubbling CO_2. Furthermore, the CO_2 responsive electrospun membranes can be used as an oil-off switch in oil/water separation (Figure 12h). Zhu et al. reported the dual-responsive wettability surface from coaxial polyaniline–polyacrylonitrile (PANI–PAN) nanofibers in response to chemical stimuli.[235] The as-prepared coaxial nanofibers show reversible switching between superhydrophobicity and superhydrophilicity on changing the pH value and redox reaction of the probe solution. These works may open up a new way of controllable biological separation systems, controllable growth of cells, and sensors fields.

5. Summary and Outlook

Electrospinning and wettability are two typical "old" fields, but almost simultaneously revivified in past two decades. Superwettability materials are dominated by a combination of suitable surface free energy with micro/nanoscale structures. Coincidently, the electrospinning technique exactly provides a simple but effective route to fabricate various nano/microstructured nanofibers with tuneable surface free energy. As a result, the combination of these two fields has ignited sparks of many interesting materials in various applications, and it is confident to predict that more innovative and influential researches will emerge in the future. In this review, we present an overview on bioinspired hierarchical structured electrospinning superwettability surfaces and their applications. Although significant achievements have been made, challenges still exist from theoretical research to materials fabrication and practical applications. First, the wetting theory mode for droplet on electrospun stereo fibers needs to be further established. For the current works of wetting theory on electrospun materials, it often directly adopted the classic wetting mechanisms that are normally used for solid rough surface. As a matter of fact, these mechanisms are not very fit to the electrospun materials because of the high curvature configuration of fibers and 3D porous structures of fibers mat. Meanwhile, the fundamental theory of electrospinning itself is insufficient because of the multiparameters and ultrafast dynamic process characteristics of electrospinning. Second, the materials fabrication, structure uniformity, mechanical strength, and productivity are still not ideal for electrospun fibers. These imperfections largely hinder the application scope of the superwettability electrospun materials. Nevertheless, everything has two sides, challenges herald opportunities. Future development of electrospinning will be achieved by multidisciplinary cooperation of chemistry, materials science, physics, electro-hydrodynamics, engineering, etc. More progressive and advanced wettability theory will be put forward. It is believed that the combination of electrospinning with superwettability systems will breed numerous creative achievements in the near future.

Acknowledgements

The authors acknowledge the National Natural Science Foundation of China (NSFC) (Grant Nos. 21774005, 21374001, 21503005, and 21433012), the National Instrumentation Program (Grant No. 2013YQ120355), the Program for New Century Excellent Talents in University of China, the Fundamental Research Funds for the Central Universities, the National Program for Support of Top-notch Young Professionals, and the 111 project (Grant No. B14009).

Conflict of Interest

The authors declare no conflict of interest.

Keywords

bioinspired fibers, electrospinning, nanofibers, superhydrophobicity, superwettability

Received: February 10, 2018
Revised: March 21, 2018
Published online: May 28, 2018

[1] M. Liu, S. Wang, L. Jiang, *Nat. Rev. Mater.* **2017**, *2*, 17036.
[2] T. Sun, L. Feng, X. Gao, L. Jiang, *Acc. Chem. Res.* **2005**, *38*, 644.
[3] S. T. Wang, K. S. Liu, X. Yao, L. Jiang, *Chem. Rev.* **2015**, *115*, 8230.
[4] T. Darmanin, F. Guittard, *J. Mater. Chem. A* **2014**, *2*, 16319.
[5] B. Wang, W. Liang, Z. Guo, W. Liu, *Chem. Soc. Rev.* **2015**, *44*, 336.
[6] A. Marmur, *Langmuir* **2004**, *20*, 3517.
[7] N. A. Patankar, *Langmuir* **2004**, *20*, 8209.
[8] W. Barthlott, C. Neinhuis, *Planta* **1997**, *202*, 1.
[9] S. G. Lee, H. S. Lim, D. Y. Lee, D. Kwak, K. Cho, *Adv. Funct. Mater.* **2013**, *23*, 547.
[10] Y. Y. Liu, X. Q. Chen, J. H. Xin, *Bioinspiration Biomimetics* **2008**, *3*, 046007.
[11] E. Bormashenko, Y. Bormashenko, T. Stein, G. Whyman, E. Bormashenko, *J. Colloids Interface Sci.* **2007**, *311*, 212.
[12] D. L. Hu, B. Chan, J. W. M. Bush, *Nature* **2003**, *424*, 663.
[13] X. Gao, L. Jiang, *Nature* **2004**, *432*, 36.
[14] X.-Q. Feng, X. Gao, Z. Wu, L. Jiang, Q.-S. Zheng, *Langmuir* **2007**, *23*, 4892.
[15] Y. Zheng, H. Bai, Z. Huang, X. Tian, F.-Q. Nie, Y. Zhao, J. Zhai, L. Jiang, *Nature* **2010**, *463*, 640.
[16] H. Bai, J. Ju, Y. Zheng, L. Jiang, *Adv. Mater.* **2012**, *24*, 2786.
[17] J. Ju, H. Bai, Y. Zheng, T. Zhao, R. Fang, L. Jiang, *Nat. Commun.* **2012**, *3*, 1247.
[18] H. Chen, P. Zhang, L. Zhang, H. Liu, Y. Jiang, D. Zhang, Z. Han, L. Jiang, *Nature* **2016**, *532*, 85.
[19] U. Bauer, T. U. Grafe, W. Federle, *J. Exp. Bot.* **2011**, *62*, 3683.
[20] A. Vilcnik, I. Jerman, A. S. Vuk, M. Kozelj, B. Orel, B. Tomsic, B. Simonic, J. Kovac, *Langmuir* **2009**, *25*, 5869.
[21] K. Tadanaga, N. Katata, T. Minami, *J. Am. Ceram. Soc.* **1997**, *80*, 3213.
[22] M. Ma, Y. Mao, M. Gupta, K. K. Gleason, G. C. Rutledge, *Macromolecules* **2005**, *38*, 9742.
[23] H. Li, X. Wang, Y. Song, Y. Liu, Q. Li, L. Jiang, D. Zhu, *Angew. Chem., Int. Ed.* **2001**, *40*, 1743.
[24] L. Shi, K. Chen, R. Du, A. Bachmatiuk, M. H. Rummeli, K. Xie, Y. Huang, Y. Zhang, Z. Liu, *J. Am. Chem. Soc.* **2016**, *138*, 6360.
[25] S. Hong, M. Minary-Jolandan, M. Naraghi, *Compos. Sci. Technol.* **2015**, *117*, 130.

[26] Q. Liu, A. A. Patel, L. Liu, *ACS Appl. Mater. Interfaces* **2014**, *6*, 8996.
[27] Y. Zhu, F. Zhang, D. Wang, X. F. Pei, W. Zhang, J. Jin, *J. Mater. Chem. A* **2013**, *1*, 5758.
[28] K.-M. Park, B.-S. Lee, J. H. Youk, J. Lee, W.-R. Yu, *ACS Appl. Mater. Interfaces* **2013**, *5*, 11115.
[29] M. S. Bobji, S. V. Kumar, A. Asthana, R. N. Govardhan, *Langmuir* **2009**, *25*, 12120.
[30] M. Jin, X. Feng, J. Xi, J. Zhai, K. Cho, L. Feng, L. Jiang, *Macromol. Rapid Commun.* **2005**, *26*, 1805.
[31] D. Rhee, W. K. Lee, T. W. Odom, *Angew. Chem., Int. Ed.* **2017**, *56*, 6523.
[32] J. Wang, Y. Zheng, F.-Q. Nie, J. Zhai, L. Jiang, *Langmuir* **2009**, *25*, 14129.
[33] S. C. Cho, Y. C. Hong, H. S. Uhm, *J. Mater. Chem.* **2007**, *17*, 232.
[34] A. Ruiz, A. Valsesia, G. Ceccone, D. Gilliland, P. Colpo, F. Rossi, *Langmuir* **2007**, *23*, 12984.
[35] N. Vourdas, A. Tserepi, E. Gogolides, *Nanotechnology* **2007**, *18*, 125304.
[36] T. Darmanin, E. T. de Givenchy, S. Amigoni, F. Guittard, *Adv. Mater.* **2013**, *25*, 1378.
[37] H.-M. Bok, T.-Y. Shin, S. Park, *Chem. Mater.* **2008**, *20*, 2247.
[38] Y. Jiang, Z. Wang, X. Yu, F. Shi, H. Xu, X. Zhang, M. Smet, W. Dehaen, *Langmuir* **2005**, *21*, 1986.
[39] N. Zhao, F. Shi, Z. Wang, X. Zhang, *Langmuir* **2005**, *21*, 4713.
[40] K. Koch, B. Bhushan, Y. C. Jung, W. Barthlott, *Soft Matter* **2009**, *5*, 1386.
[41] J. T. Woodward, H. Gwin, D. K. Schwartz, *Langmuir* **2000**, *16*, 2957.
[42] K. Chen, S. Zhou, L. Wu, *ACS Nano* **2015**, *10*, 1386.
[43] A. M. Higgins, R. A. L. Jones, *Nature* **2000**, *404*, 476.
[44] P. S. Brown, B. Bhushan, *Sci. Rep.* **2015**, *5*, 8701.
[45] F. Shi, Z. Wang, X. Zhang, *Adv. Mater.* **2005**, *17*, 1005.
[46] M. Sun, C. Luo, L. Xu, H. Ji, Q. Ouyang, D. Yu, Y. Chen, *Langmuir* **2005**, *21*, 8978.
[47] L. Feng, S. Li, H. Li, J. Zhai, Y. Song, L. Jiang, D. Zhu, *Angew. Chem., Int. Ed.* **2002**, *41*, 1221.
[48] L. Zhang, Z. Zhou, B. Cheng, J. M. DeSimone, E. T. Samulski, *Langmuir* **2006**, *22*, 8576.
[49] W. Zhang, Z. Shi, F. Zhang, X. Liu, J. Jin, L. Jiang, *Adv. Mater.* **2013**, *25*, 2071.
[50] W. Zhang, Y. Zhu, X. Liu, D. Wang, J. Li, L. Jiang, J. Jin, *Angew. Chem., Int. Ed.* **2014**, *53*, 856.
[51] L. Jiang, Y. Zhao, J. Zhai, *Angew. Chem., Int. Ed.* **2004**, *43*, 4338.
[52] M. L. Ma, R. M. Hill, J. L. Lowery, S. V. Fridrikh, G. C. Rutledge, *Langmuir* **2005**, *21*, 5549.
[53] H. Tang, H. Wang, J. He, *J. Phys. Chem. C* **2009**, *113*, 14220.
[54] A. Greiner, J. H. Wendorff, *Angew. Chem., Int. Ed.* **2007**, *46*, 5670.
[55] D. Li, Y. Wang, Y. Xia, *Adv. Mater.* **2004**, *16*, 361.
[56] D. H. Reneker, A. L. Yarin, *Polymer* **2008**, *49*, 2387.
[57] F. Anton, *US Patent US1975504*, **1934**.
[58] H. Simons, *US Patent US3280229*, **1966**.
[59] P. Baumgarten, *J. Colloids Interface Sci.* **1971**, *36*, 71.
[60] D. Reneker, I. Chun, *Nanotechnology* **1996**, *7*, 216.
[61] J. Doshi, D. H. Reneker, *J. Electrostat.* **1995**, *35*, 151.
[62] H. Fong, I. Chun, D. H. Reneker, *Polymer* **1999**, *40*, 4585.
[63] S. Koombhongse, W. X. Liu, D. H. Reneker, *J. Polym. Sci., Polym. Phys.* **2001**, *39*, 2598.
[64] H. Dong, N. Wang, L. Wang, H. Bai, J. Wu, Y. Zheng, Y. Zhao, L. Jiang, *ChemPhysChem* **2012**, *13*, 1153.
[65] M. Bognitzki, W. Czado, T. Frese, A. Schaper, M. Hellwig, M. Steinhart, A. Greiner, J. H. Wendorff, *Adv. Mater.* **2001**, *13*, 70.
[66] Z. Liu, D. D. Sun, P. Guo, J. O. Leckie, *Nano Lett.* **2007**, *7*, 1081.
[67] D. Li, Y. N. Xia, *Nano Lett.* **2004**, *4*, 933.
[68] H. Chen, N. Wang, J. Di, Y. Zhao, Y. Song, L. Jiang, *Langmuir* **2010**, *26*, 11291.
[69] R. Jin, Y. Yang, Y. Xing, L. Chen, S. Song, R. Jin, *ACS Nano* **2014**, *8*, 3664.
[70] H. Chen, J. Di, N. Wang, H. Dong, J. Wu, Y. Zhao, J. Yu, L. Jiang, *Small* **2011**, *7*, 1779.
[71] C. Niu, J. Meng, X. Wang, C. Han, M. Yan, K. Zhao, X. Xu, W. Ren, Y. Zhao, L. Xu, Q. Zhang, D. Zhao, L. Mai, *Nat. Commun.* **2015**, *6*, 7402.
[72] H. Fong, W. Liu, C.-S. Wang, R. A. Vaia, *Polymer* **2002**, *43*, 775.
[73] D. Li, Y. N. Xia, *Adv. Mater.* **2004**, *16*, 1151.
[74] R. Jaeger, M. M. Bergshoef, C. M. I. Batlle, H. Schönherr, G. Julius Vancso, *Macromol. Symp.* **1998**, *127*, 141.
[75] S. Megelski, J. S. Stephens, D. B. Chase, J. F. Rabolt, *Macromolecules* **2002**, *35*, 8456.
[76] J. Zheng, A. He, J. Li, J. Xu, C. C. Han, *Polymer* **2006**, *47*, 7095.
[77] A. V. Bazilevsky, A. L. Yarin, C. M. Megaridis, *Langmuir* **2007**, *23*, 2311.
[78] I. G. Loscertales, A. Barrero, I. Guerrero, R. Cortijo, M. Marquez, A. M. Ganan-Calvo, *Science* **2002**, *295*, 1695.
[79] J. H. Yu, S. V. Fridrikh, G. C. Rutledge, *Adv. Mater.* **2004**, *16*, 1562.
[80] D. Li, J. T. McCann, Y. N. Xia, *Small* **2005**, *1*, 83.
[81] Z. Sun, E. Zussman, A. L. Yarin, J. H. Wendorff, A. Greiner, *Adv. Mater.* **2003**, *15*, 1929.
[82] J. T. McCann, D. Li, Y. Xia, *J. Mater. Chem.* **2005**, *15*, 735.
[83] I. G. Loscertales, A. Barrero, M. Márquez, R. Spretz, R. Velarde-Ortiz, G. Larsen, *J. Am. Chem. Soc.* **2004**, *126*, 5376.
[84] Z. C. Sun, E. Zussman, A. L. Yarin, J. H. Wendorff, A. Greiner, *Adv. Mater.* **2003**, *15*, 1929.
[85] Y. Zhao, X. Cao, L. Jiang, *J. Am. Chem. Soc.* **2007**, *129*, 764.
[86] T. Zhao, Z. Liu, K. Nakata, S. Nishimoto, T. Murakami, Y. Zhao, L. Jiang, A. Fujishima, *J. Mater. Chem.* **2010**, *20*, 5095.
[87] G. Yazgan, A. M. Popa, R. M. Rossi, K. Maniura-Weber, J. Puigmartí-Luis, D. Crespy, G. Fortunato, *Polymer* **2015**, *66*, 268.
[88] J. T. McCann, M. Marquez, Y. Xia, *J. Am. Chem. Soc.* **2006**, *128*, 1436.
[89] M. Peng, D. Li, L. Shen, Y. Chen, Q. Zheng, H. Wang, *Langmuir* **2006**, *22*, 9368.
[90] N. Wang, J.-N. Zhang, H.-Y. Chen, Y. Zhao, X.-Y. Cao, Q.-L. Yang, Y.-M. Ma, L. Jiang, *Chem. J. Chin.* **2010**, *31*, 227.
[91] S. Peng, G. Jin, L. Li, K. Li, M. Srinivasan, S. Ramakrishna, J. Chen, *Chem. Soc. Rev.* **2016**, *45*, 1225.
[92] J. Xu, C. Liu, P. C. Hsu, K. Liu, R. Zhang, Y. Liu, Y. Cui, *Nano Lett.* **2016**, *16*, 1270.
[93] T. H. Hwang, Y. M. Lee, B.-S. Kong, J.-S. Seo, J. W. Choi, *Nano Lett.* **2012**, *12*, 802.
[94] S. Mukherjee, J. Reddy Venugopal, R. Ravichandran, S. Ramakrishna, M. Raghunath, *Adv. Funct. Mater.* **2011**, *21*, 2291.
[95] H. Bellanger, T. Darmanin, E. Taffin de Givenchy, F. Guittard, *Chem. Rev.* **2014**, *114*, 2694.
[96] Y. Tian, B. Su, L. Jiang, *Adv. Mater.* **2014**, *26*, 6872.
[97] B. Su, Y. Tian, L. Jiang, *J. Am. Chem. Soc.* **2016**, *138*, 1727.
[98] T. Young, *Philos. Trans. R. Soc. London* **1805**, *95*, 65.
[99] A. Lafuma, D. Quere, *Nat. Mater.* **2003**, *2*, 457.
[100] R. N. Wenzel, *Ind. Eng. Chem.* **1936**, *28*, 988.
[101] A. B. D. Cassie, S. Baxter, *Trans. Faraday Soc.* **1944**, *40*, 546.
[102] D. Quéré, *Annu. Rev. Fluid Mech.* **1999**, *31*, 347.
[103] E. Lorenceau, C. Clanet, D. Quere, *J. Colloids Interface Sci.* **2004**, *279*, 192.
[104] K. Piroird, C. Clanet, E. Lorenceau, D. Quere, *J. Colloids Interface Sci.* **2009**, *334*, 70.
[105] J. P. Youngblood, T. J. McCarthy, *Macromolecules* **1999**, *32*, 6800.
[106] D. Tian, X. Zhang, Y. Tian, Y. Wu, X. Wang, J. Zhai, L. Jiang, *J. Mater. Chem.* **2012**, *22*, 19652.
[107] L. Rayleigh, *Proc. London Math. Soc.* **1878**, *10*, 4.
[108] P. P. Bhat, S. Appathurai, M. T. Harris, M. Pasquali, G. H. McKinley, O. A. Basaran, *Nat. Phys.* **2010**, *6*, 625.
[109] L. Élise, D. Quéré, *J. Fluid Mech.* **2004**, *510*, 29.
[110] Q. Wang, B. Su, H. Liu, L. Jiang, *Adv. Mater.* **2014**, *26*, 4889.

[111] L. Feng, Y. Zhang, J. Xi, Y. Zhu, N. Wang, F. Xia, L. Jiang, *Langmuir* **2008**, *24*, 4114.
[112] G. Gong, J. Wu, J. Liu, N. Sun, Y. Zhao, L. Jiang, *J. Mater. Chem.* **2012**, *22*, 8257.
[113] A. R. Parker, C. R. Lawrence, *Nature* **2001**, *414*, 33.
[114] C. S. Sharma, A. Sharma, M. Madou, *Langmuir* **2010**, *26*, 2218.
[115] J. Lin, Y. Cai, X. Wang, B. Ding, J. Yu, M. Wang, *Nanoscale* **2011**, *3*, 1258.
[116] X. Li, B. Ding, J. Lin, J. Yu, G. Sun, *J. Phys. Chem. C* **2009**, *113*, 20452.
[117] Y. Xue, H. Wang, D. Yu, L. Feng, L. Dai, X. Wang, T. Lin, *Chem. Commun.* **2009**, *42*, 6418.
[118] H. Wu, R. Zhang, Y. Sun, D. Lin, Z. Sun, W. Pan, P. Downs, *Soft Matter* **2008**, *4*, 2429.
[119] W. Barthlott, C. Neinhuis, *Ann. Bot.* **1997**, *79*, 667.
[120] L. Feng, S. Li, Y. Li, H. Li, L. Zhang, J. Zhai, Y. Song, B. Liu, L. Jiang, D. Zhu, *Adv. Mater.* **2002**, *14*, 1857.
[121] K. Acatay, E. Simsek, C. Ow-Yang, Y. Z. Menceloglu, *Angew. Chem., Int. Ed.* **2004**, *43*, 5210.
[122] Y. Zhu, J. C. Zhang, Y. M. Zheng, Z. B. Huang, L. Feng, L. Jiang, *Adv. Funct. Mater.* **2006**, *16*, 568.
[123] H. Yoon, J. H. Park, G. H. Kim, *Macromol. Rapid Commun.* **2010**, *31*, 1435.
[124] F. Zhao, X. Wang, B. Ding, J. Lin, J. Hu, Y. Si, J. Yu, G. Sun, *RSC Adv.* **2011**, *1*, 1482.
[125] M. Kang, R. Jung, H.-S. Kim, H.-J. Jin, *Colloids Surf., A* **2008**, *313*, 411.
[126] M. Ma, M. Gupta, Z. Li, L. Zhai, K. K. Gleason, R. E. Cohen, M. F. Rubner, G. C. Rutledge, *Adv. Mater.* **2007**, *19*, 255.
[127] G. Gong, J. Wu, X. Jin, L. Jiang, *Macromol. Mater. Eng.* **2015**, *300*, 1057.
[128] W. S. Y. Wong, N. Nasiri, G. Liu, N. Rumsey-Hill, V. S. J. Craig, D. R. Nisbet, A. Tricoli, *Adv. Mater. Interfaces* **2015**, *2*, 1500071.
[129] Y. Zheng, X. Gao, L. Jiang, *Soft Matter* **2007**, *3*, 178.
[130] C. Liu, J. Ju, Y. Zheng, L. Jiang, *ACS Nano* **2014**, *8*, 1321.
[131] R. P. Garrod, L. G. Harris, W. C. E. Schofield, J. McGettrick, L. J. Ward, D. O. H. Teare, J. P. S. Badyal, *Langmuir* **2007**, *23*, 689.
[132] Y. M. Hou, M. Yu, X. M. Chen, Z. K. Wang, S. H. Yao, *ACS Nano* **2015**, *9*, 71.
[133] Z. Yu, F. F. Yun, Y. Wang, L. Yao, S. Dou, K. Liu, L. Jiang, X. Wang, *Small* **2017**, *13*, 1701403.
[134] Z.-Z. Gu, H.-M. Wei, R.-Q. Zhang, G.-Z. Han, C. Pan, H. Zhang, X.-J. Tian, Z.-M. Chen, *Appl. Phys. Lett.* **2005**, *86*, 201915.
[135] R. J. Kennedy, *Nature* **1970**, *227*, 736.
[136] A. Tuteja, W. Choi, J. M. Mabry, G. H. McKinley, R. E. Cohen, *Proc. Natl. Acad. Sci. USA* **2008**, *105*, 18200.
[137] X. Deng, L. Mammen, H.-J. Butt, D. Vollmer, *Science* **2012**, *335*, 67.
[138] T. Darmanin, F. Guittard, *J. Am. Chem. Soc.* **2009**, *131*, 7928.
[139] Z. Xue, S. Wang, L. Lin, L. Chen, M. Liu, L. Feng, L. Jiang, *Adv. Mater.* **2011**, *23*, 4270.
[140] X. Yao, J. Gao, Y. Song, L. Jiang, *Adv. Funct. Mater.* **2011**, *21*, 4270.
[141] H. Zhao, K.-Y. Law, *Langmuir* **2012**, *28*, 11821.
[142] K. Liu, Y. Tian, L. Jiang, *Prog. Mater. Sci.* **2013**, *58*, 503.
[143] W. S. Y. Wong, G. Y. Liu, N. Nasiri, C. L. Hao, Z. K. Wang, A. Tricoli, *ACS Nano* **2017**, *11*, 587.
[144] L. Hou, L. Wang, N. Wang, F. Guo, J. Liu, Y. Chen, J. Liu, Y. Zhao, L. Jiang, *NPG Asia Mater.* **2016**, *8*, e334.
[145] D. Han, A. J. Steckl, *Langmuir* **2009**, *25*, 9454.
[146] A. Tuteja, W. Choi, M. Ma, J. M. Mabry, S. A. Mazzella, G. C. Rutledge, G. H. McKinley, R. E. Cohen, *Science* **2007**, *318*, 1618.
[147] Y. Cai, L. Lin, Z. Xue, M. Liu, S. Wang, L. Jiang, *Adv. Funct. Mater.* **2014**, *24*, 808.
[148] M. Liu, S. Wang, Z. Wei, Y. Song, L. Jiang, *Adv. Mater.* **2009**, *21*, 665.
[149] T.-S. Wong, S. H. Kang, S. K. Y. Tang, E. J. Smythe, B. D. Hatton, A. Grinthal, J. Aizenberg, *Nature* **2011**, *477*, 443.
[150] M. Jin, S. Li, J. Wang, Z. Xue, M. Liao, S. Wang, *Chem. Commun.* **2012**, *48*, 11745.
[151] X. Tian, V. Jokinen, J. Li, J. Sainio, R. H. A. Ras, *Adv. Mater.* **2016**, *28*, 10652.
[152] L. Wang, Y. Zhao, J. Wang, X. Hong, J. Zhai, L. Jiang, F. Wang, *Appl. Surf. Sci.* **2009**, *255*, 4944.
[153] R. S. Kurusu, N. R. Demarquette, *Langmuir* **2015**, *31*, 5495.
[154] L. D. Tijing, M. T. G. Ruelo, A. Amarjargal, H. R. Pant, C.-H. Park, D. W. Kim, C. S. Kim, *Chem. Eng. J.* **2012**, *197*, 41.
[155] K. Yoon, K. Kim, X. F. Wang, D. F. Fang, B. S. Hsiao, B. Chu, *Polymer* **2006**, *47*, 2434.
[156] J. Drelich, E. Chibowski, D. D. Meng, K. Terpilowski, *Soft Matter* **2011**, *7*, 9804.
[157] Y. Zhu, J. C. Zhang, J. Zhai, L. Jiang, *Thin Solid Films* **2006**, *510*, 271.
[158] A. Abdal-hay, H. R. Pant, J. K. Lim, *Eur. Polym. J.* **2013**, *49*, 1314.
[159] T. J. Crone, M. Tolstoy, *Science* **2010**, *330*, 634.
[160] J. Ge, L. A. Shi, Y. C. Wang, H. Y. Zhao, H. B. Yao, Y. B. Zhu, Y. Zhang, H. W. Zhu, H. A. Wu, S. H. Yu, *Nat. Nanotechnol.* **2017**, *12*, 434.
[161] Q. Zhu, Q. Pan, F. Liu, *J. Phys. Chem. C* **2011**, *115*, 17464.
[162] X. Gui, J. Wei, K. Wang, A. Cao, H. Zhu, Y. Jia, Q. Shu, D. Wu, *Adv. Mater.* **2010**, *22*, 617.
[163] J. Yuan, X. Liu, O. Akbulut, J. Hu, S. L. Suib, J. Kong, F. Stellacci, *Nat. Nanotechnol.* **2008**, *3*, 332.
[164] N. Cervin, C. Aulin, P. Larsson, L. Wågberg, *Cellulose* **2012**, *19*, 401.
[165] A. B. Nordvik, J. L. Simmons, K. R. Bitting, A. Lewis, T. Strøm-Kristiansen, *Spill Sci. Technol. Bull.* **1996**, *3*, 107.
[166] J. Wu, N. Wang, L. Wang, H. Dong, Y. Zhao, L. Jiang, *ACS Appl. Mater. Interfaces* **2012**, *4*, 3207.
[167] J. Wu, N. Wang, Y. Zhao, L. Jiang, *Nanoscale* **2015**, *7*, 2625.
[168] J. Lin, F. Tian, Y. Shang, F. Wang, B. Ding, J. Yu, Z. Guo, *Nanoscale* **2013**, *5*, 2745.
[169] M. H. Tai, B. Y. L. Tan, J. Juay, D. D. Sun, J. O. Leckie, *Chem. - Eur. J.* **2015**, *21*, 5395.
[170] J. Gao, X. Yao, Y. Zhao, L. Jiang, *Small* **2013**, *9*, 2515.
[171] M. Jin, J. Wang, X. Yao, M. Liao, Y. Zhao, L. Jiang, *Adv. Mater.* **2011**, *23*, 2861.
[172] Z. G. Lei, C. Y. Li, B. H. Chen, *Sep. Purif. Rev.* **2003**, *32*, 121.
[173] S. Gunawan, N. S. Kasim, Y.-H. Ju, *Sep. Purif. Technol.* **2008**, *60*, 128.
[174] J. Liu, L. Wang, F. Guo, L. Hou, Y. Chen, J. Liu, N. Wang, Y. Zhao, L. Jiang, *J. Mater. Chem. A* **2016**, *4*, 4365.
[175] P. Kajitvichyanukul, Y.-T. Hung, L. Wang, in *Advanced Physicochemical Treatment Processes*, Vol. *4* (Eds: L. Wang, Y.-T. Hung, N. Shammas), Humana Press, Totowa, NJ **2006**, Chap. 16.
[176] L. Xu, N. Liu, Y. Cao, F. Lu, Y. Chen, X. Zhang, L. Feng, Y. Wei, *ACS Appl. Mater. Interfaces* **2014**, *6*, 13324.
[177] K. He, H. Duan, G. Y. Chen, X. Liu, W. Yang, D. Wang, *ACS Nano* **2015**, *9*, 9188.
[178] Z. Xu, Y. Zhao, H. Wang, X. Wang, T. Lin, *Angew. Chem., Int. Ed.* **2015**, *54*, 4527.
[179] Z. Cheng, J. Wang, H. Lai, Y. Du, R. Hou, C. Li, N. Zhang, K. Sun, *Langmuir* **2015**, *31*, 1393.
[180] Y. Shang, Y. Si, A. Raza, L. Yang, X. Mao, B. Ding, J. Yu, *Nanoscale* **2012**, *4*, 7847.
[181] M. H. Tai, P. Gao, B. Y. L. Tan, D. D. Sun, J. O. Leckie, *ACS Appl. Mater. Interfaces* **2014**, *6*, 9393.
[182] X. Li, M. Wang, C. Wang, C. Cheng, X. Wang, *ACS Appl. Mater. Interfaces* **2014**, *6*, 15272.
[183] S. Qiu, L. Hou, J. Liu, F. Guo, Y. Zhang, L. Zhang, K. Liu, N. Wang, Y. Zhao, *RSC Adv.* **2017**, *7*, 19434.

[184] L. F. Wang, S. Y. Yang, J. Wang, C. F. Wang, L. Chen, *Mater. Lett.* **2011**, *65*, 869.
[185] M. W. Lee, S. An, S. S. Latthe, C. Lee, S. Hong, S. S. Yoon, *ACS Appl. Mater. Interfaces* **2013**, *5*, 10597.
[186] X. Tang, Y. Si, J. Ge, B. Ding, L. Liu, G. Zheng, W. Luo, J. Yu, *Nanoscale* **2013**, *5*, 11657.
[187] J. Liu, N. Wang, L.-J. Yu, A. Karton, W. Li, W. Zhang, F. Guo, L. Hou, Q. Cheng, L. Jiang, D. A. Weitz, Y. Zhao, *Nat. Commun.* **2017**, *8*, 2011.
[188] S. J. Gao, Z. Shi, W. B. Zhang, F. Zhang, J. Jin, *ACS Nano* **2014**, *8*, 6344.
[189] W. Zhang, N. Liu, Y. Cao, Y. Chen, L. Xu, X. Lin, L. Feng, *Adv. Mater.* **2015**, *27*, 7349.
[190] Z. Wang, G. Liu, S. Huang, *Angew. Chem., Int. Ed.* **2016**, *55*, 14610.
[191] Y. Chen, N. Wang, F. Guo, L. Hou, J. Liu, J. Liu, Y. Xu, Y. Zhao, L. Jiang, *J. Mater. Chem. A* **2016**, *4*, 12014.
[192] M. Tao, L. Xue, F. Liu, L. Jiang, *Adv. Mater.* **2014**, *26*, 2943.
[193] Y. Zhang, Y. Chen, L. Hou, F. Guo, J. Liu, S. Qiu, Y. Xu, N. Wang, Y. Zhao, *J. Mater. Chem. A* **2017**, *5*, 16134.
[194] W. Lv, Q. Mei, J. Xiao, M. Du, Q. Zheng, *Adv. Funct. Mater.* **2017**, *27*, 1704293.
[195] J. Ge, D. Zong, Q. Jin, J. Yu, B. Ding, *Adv. Funct. Mater.* **2018**, *28*, 1705051.
[196] Y. Si, Q. Fu, X. Wang, J. Zhu, J. Yu, G. Sun, B. Ding, *ACS Nano* **2015**, *9*, 3791.
[197] S. Yang, Y. Si, Q. Fu, F. Hong, J. Yu, S. S. Al-Deyab, M. El-Newehy, B. Ding, *Nanoscale* **2014**, *6*, 12445.
[198] Y. Si, J. Yu, X. Tang, J. Ge, B. Ding, *Nat. Commun.* **2014**, *5*, 5802.
[199] J. Liu, L. Wang, N. Wang, F. Guo, L. Hou, Y. Chen, J. Liu, Y. Zhao, L. Jiang, *Small* **2017**, *13*, 1600499.
[200] F. Chen, Y. Lu, X. Liu, J. Song, G. He, M. K. Tiwari, C. J. Carmalt, I. P. Parkin, *Adv. Funct. Mater.* **2017**, *27*, 1702926.
[201] L. Wang, Y. Zhao, Y. Tian, L. Jiang, *Angew. Chem., Int. Ed.* **2015**, *54*, 14732.
[202] Y. Wang, J. Di, L. Wang, X. Li, N. Wang, B. Wang, Y. Tian, L. Jiang, J. Yu, *Nat. Commun.* **2017**, *8*, 575.
[203] S. Zhang, J. Huang, Z. Chen, Y. Lai, *Small* **2017**, *13*, 1602992.
[204] J. Ju, Y. Zheng, L. Jiang, *Acc. Chem. Res.* **2014**, *47*, 2342.
[205] X. Tian, Y. Chen, Y. Zheng, H. Bai, L. Jiang, *Adv. Mater.* **2011**, *23*, 5486.
[206] Y. Hou, Y. Chen, Y. Xue, L. Wang, Y. Zheng, L. Jiang, *Soft Matter* **2012**, *8*, 11236.
[207] X. Tian, H. Bai, Y. Zheng, L. Jiang, *Adv. Funct. Mater.* **2011**, *21*, 1398.
[208] M. Du, Y. Zhao, Y. Tian, K. Li, L. Jiang, *Small* **2016**, *12*, 1000.
[209] Y.-X. Huang, Z. Wang, J. Jin, S. Lin, *Environ. Sci. Technol.* **2017**, *51*, 13304.
[210] H.-C. Yang, J. Hou, V. Chen, Z.-K. Xu, *Angew. Chem., Int. Ed.* **2016**, *55*, 13398.
[211] X. Tian, H. Jin, J. Sainio, R. H. A. Ras, O. Ikkala, *Adv. Funct. Mater.* **2014**, *24*, 6023.
[212] Y. Kong, Y. Liu, J. H. Xin, *J. Mater. Chem.* **2011**, *21*, 17978.
[213] J. B. You, Y. Yoo, M. S. Oh, S. G. Im, *ACS Appl. Mater. Interfaces* **2014**, *6*, 4005.
[214] L. Hu, S. Gao, Y. Zhu, F. Zhang, L. Jiang, J. Jin, *J. Mater. Chem. A* **2015**, *3*, 23477.
[215] H. S. Lim, S. H. Park, S. H. Koo, Y.-J. Kwark, E. L. Thomas, Y. Jeong, J. H. Cho, *Langmuir* **2010**, *26*, 19159.
[216] H. X. Wang, H. Zhou, H. T. Niu, J. Zhang, Y. Du, T. Lin, *Adv. Mater. Interfaces* **2015**, *2*, 1400506.
[217] H. Wang, H. Zhou, W. Yang, Y. Zhao, J. Fang, T. Lin, *ACS Appl. Mater. Interfaces* **2015**, *7*, 22874.
[218] H. Wang, J. Ding, L. Dai, X. Wang, T. Lin, *J. Mater. Chem.* **2010**, *20*, 7938.
[219] J. Wu, N. Wang, L. Wang, H. Dong, Y. Zhao, L. Jiang, *Soft Matter* **2012**, *8*, 5996.
[220] K. Ichimura, S.-K. Oh, M. Nakagawa, *Science* **2000**, *288*, 1624.
[221] J. Lahann, S. Mitragotri, T. N. Tran, H. Kaido, J. Sundaram, I. S. Choi, S. Hoffer, G. A. Somorjai, R. Langer, *Science* **2003**, *299*, 371.
[222] T. P. Russell, *Science* **2002**, *297*, 964.
[223] S. Minko, M. Müller, M. Motornov, M. Nitschke, K. Grundke, M. Stamm, *J. Am. Chem. Soc.* **2003**, *125*, 3896.
[224] X. Feng, L. Feng, M. Jin, J. Zhai, L. Jiang, D. Zhu, *J. Am. Chem. Soc.* **2004**, *126*, 62.
[225] H. S. Lim, J. T. Han, D. Kwak, M. Jin, K. Cho, *J. Am. Chem. Soc.* **2006**, *128*, 14458.
[226] T. Sun, G. Wang, L. Feng, B. Liu, Y. Ma, L. Jiang, D. Zhu, *Angew. Chem., Int. Ed.* **2004**, *43*, 357.
[227] X. Yu, Z. Q. Wang, Y. G. Jiang, F. Shi, X. Zhang, *Adv. Mater.* **2005**, *17*, 1289.
[228] N. Wang, Y. Zhao, L. Jiang, *Macromol. Rapid Commun.* **2008**, *29*, 485.
[229] S.-Y. Gu, Z.-M. Wang, J.-B. Li, J. Ren, *Macromol. Mater. Eng.* **2010**, *295*, 32.
[230] M. Chen, M. Dong, R. Havelund, V. R. Regina, R. L. Meyer, F. Besenbacher, P. Kingshott, *Chem. Mater.* **2010**, *22*, 4214.
[231] M. Chen, F. Besenbacher, *ACS Nano* **2011**, *5*, 1549.
[232] M. W. Lee, S. An, B. Joshi, S. S. Latthe, S. S. Yoon, *ACS Appl. Mater. Interfaces* **2013**, *5*, 1232.
[233] Y. Wang, C. Lai, X. Wang, Y. Liu, H. Hu, Y. Guo, K. Ma, B. Fei, J. H. Xin, *ACS Appl. Mater. Interfaces* **2016**, *8*, 25612.
[234] H. Che, M. Huo, L. Peng, T. Fang, N. Liu, L. Feng, Y. Wei, J. Yuan, *Angew. Chem., Int. Ed.* **2015**, *54*, 8934.
[235] Y. Zhu, L. Feng, F. Xia, J. Zhai, M. Wan, L. Jiang, *Macromol. Rapid Commun.* **2007**, *28*, 1135.
[236] P. Li, Y. Qiao, L. Zhao, D. Yao, H. Sun, Y. Hou, S. Li, Q. Li, *Marine Pollution Bulletin* **2015**, *93*, 75.